This Accepted Manuscript has not been copyedited and formatted. The final version may differ from this version.

JNeurosci
THE JOURNAL OF NEUROSCIENCE

Research Articles: Development/Plasticity/Repair

Effects of selective deafferentation on the discharge characteristics of medial rectus motoneurons

Rosendo G. Hernández, Beatriz Benítez-Temiño, Camilo J. Morado-Díaz, María América Davis-López de Carrizosa, Rosa R. de la Cruz and Angel M. Pastor

Dpt. Fisiología, Universidad de Sevilla, Avda. Reina Mercedes 6, 41012 Sevilla, Spain.

DOI: 10.1523/JNEUROSCI.1391-17.2017

Received: 22 May 2017

Revised: 11 July 2017

Accepted: 6 August 2017

Published: 21 August 2017

Author contributions: R.G.H., B.B.-T., C.J.M.-D., and A.M.P. performed research; R.G.H. and M.A.D.-L.d.C. analyzed data; B.B.-T., R.d.l.C., and A.M.P. designed research; B.B.-T., R.d.l.C., and A.M.P. wrote the paper.

Conflict of Interest: The authors declare no competing financial interests.

This work was supported by MICINN-FEDER Grants BFU2015-64515-P and BFU2012-33975. RGH was a fellowship holder of the Universidad de Sevilla. Imaging studies were performed at CITIUS from Universidad de Sevilla.

Corresponding author: Angel M. Pastor, Departamento de Fisiología, Universidad de Sevilla, Avda. Reina Mercedes 6, 41012 Sevilla, Spain; ampastor@us.es

Cite as: J. Neurosci ; 10.1523/JNEUROSCI.1391-17.2017

Alerts: Sign up at www.jneurosci.org/cgi/alerts to receive customized email alerts when the fully formatted version of this article is published.

Accepted manuscripts are peer-reviewed but have not been through the copyediting, formatting, or proofreading process.

Copyright © 2017 the authors

JNeurosci Accepted Manuscript

JNeurosci Accepted Manuscript

Effects of selective deafferentation on the discharge characteristics of medial rectus motoneurons

Abbreviated title: Effects of deafferentation on extraocular motoneurons

Authors: Rosendo G.Hernández*, Beatriz Benítez-Temiño*, Camilo J. Morado-Díaz, María América Davis-López de Carrizosa, Rosa R. de la Cruz, Angel M. Pastor.

Affiliations: Dpt. Fisiología, Universidad de Sevilla, Avda. Reina Mercedes 6, 41012 Sevilla, Spain.

Corresponding author: Angel M. Pastor, Departamento de Fisiología, Universidad de Sevilla, Avda. Reina Mercedes 6, 41012 Sevilla, Spain; ampastor@us.es

Nº Pages: 45

Nº Figures: 10

Nº tables: 0

Nº words in the abstract: 247

Nº words in the introduction: 579

Nº words in the discussion: 1500

*Co-first authors

Conflict of interests: The authors declare no competing financial interests.

Acknowledgements: This work was supported by MICINN-FEDER Grants BFU2015-64515-P and BFU2012-33975. RGH was a fellowship holder of the Universidad de Sevilla. Imaging studies were performed at CITIUS from Universidad de Sevilla.

JNeurosci Accepted Manuscript

ABSTRACT

Medial rectus motoneurons receive two main pontine inputs: abducens internuclear neurons, whose axons course through the medial longitudinal fascicle (MLF), and neurons in the lateral vestibular nucleus, whose axons project through the ascending tract of Deiters (ATD). Abducens internuclear neurons are responsible for conjugate gaze in the horizontal plane, whereas ATD neurons provide medial rectus motoneurons with a vestibular input comprising mainly head velocity.

In order to reveal the relative contribution of each input to the oculomotor physiology, single-unit recordings from medial rectus motoneurons were carried out in the control situation and after selective deafferentation from cats with unilateral transection of either the MLF or the ATD.

Both MLF and ATD transection produced similar short-term alterations in medial rectus motoneuron firing pattern, which were more drastic in MLF animals. However, long-term recordings revealed important differences between the two types of lesion. Thus, while the effects of MLF section were permanent, two months after ATD lesion all motoneuronal firing parameters were similar to control. These findings indicated a more relevant role of the MLF pathway in driving motoneuronal firing, and evidenced compensatory mechanisms following ATD lesion. Confocal immunocytochemistry revealed that MLF transection produced also a higher loss of synaptic boutons, mainly at the dendritic level. Moreover, two months after ATD transection, we observed an increase in synaptic coverage around motoneuron cell bodies as compared with short-term data, indicative of a synaptogenic compensatory mechanism of the abducens internuclear pathway that could lead to the observed firing and morphological recovery.

JNeurosci Accepted Manuscript

SIGNIFICANCE STATEMENT

Eye movements rely on multiple neuronal circuits for appropriate performance. The abducens internuclear pathway through the MLF and the vestibular neurons through the ATD are a dual system that supports the firing of medial rectus motoneurons. We report the effect of sectioning the MLF or the ATD pathway on the firing of medial rectus motoneurons, as well as the plastic mechanisms by which one input compensates for the lack of the other. This work shows that while the effects of MLF transection are permanent, the ATD section produces transitory effects. A mechanism based on axonal sprouting and occupancy of the vacant synaptic space due to deafferentation is the base for the mechanism of compensation on the medial rectus motoneuron.

INTRODUCTION

Lateral and medial rectus extraocular muscles constitute the agonist/antagonistic pair involved in the generation of horizontal gaze. Their parent motoneurons lie in the abducens and oculomotor nuclei, respectively (Büttner-Ennever, 2006). Both types of motoneurons display a similar tonic-phasic discharge pattern during eye fixations and saccades, respectively (Delgado-García et al., 1988a; Fuchs et al., 1988; de la Cruz et al., 1989; Pastor et al., 1991). Despite their comparable firing pattern and parallel function in conjugate eye movements, the synaptic organization of lateral rectus and medial rectus motoneurons is quite different. Thus, abducens motoneurons receive direct afferents mainly from a threefold system that conveys signals associated to either saccades (pontomedullary reticular formation), slow phases of the vestibular nystagmus (medial vestibular nucleus) or eye fixations (prepositus hypoglossi nuclei; Hikosaka et

JNeurosci Accepted Manuscript

al., 1978; Grantyn et al., 1980; Igusa et al., 1980; McCrea et al., 1980; McCrea and Baker, 1985; Escudero and Delgado-García, 1988; Büttner-Ennever, 2006).

On the contrary, the main input to medial rectus motoneurons conveys an already integrated signal originated at the abducens internuclear neurons, which project contralaterally through the medial longitudinal fascicle (MLF) and mediate horizontal conjugate gaze (Highstein and Baker, 1978; Carpenter and Carleton, 1983; Delgado-García et al. 1988b; McCrea et al., 1986; González-Forero et al., 2005; Büttner-Ennever, 2006). The importance of this pathway has been revealed in lesion experiments where the MLF has been sectioned, inducing the syndrome of internuclear ophthalmoplegia, which involves the disturbance of versional horizontal eye movements, the abduction position of the ipsilateral eye at rest, and the inability of this eye to cross into the nasal visual hemifield, except during convergence movements (Carpenter and McMasters, 1963; Highstein, 1977; Highstein and Baker, 1978; de la Cruz et al., 2000).

The second source of pontine afferences to medial rectus motoneurons arise in the ventral portion of the lateral vestibular nucleus and project ipsilaterally through the ascending tract of Deiters (ATD), which courses lateral to the MLF (Baker and Highstein, 1978; Furuya and Markham, 1981; Büttner-Ennever, 2006). The role of this input has been interpreted as redundant since it encodes head velocity and eye position signals that are also carried by abducens internuclear neurons (Reisine and Highstein, 1979; Reisine et al., 1981). However, there are striking differences between MLF *versus* ATD pathways, concerning the strategic somatodendritic distribution of their respective synaptic terminals. In particular, ATD neurons terminate preferentially over the soma and proximal dendrites of medial rectus motoneurons, whereas the majority of abducens internuclear synaptic endings contact distal dendrites (Nguyen et al., 1999), therefore

JNeurosci Accepted Manuscript

pointing to a crucial role of the ATD pathway in the processing of the information coming from abducens internuclear neurons (Nguyen et al., 1999).

In the present work, we have performed the unilateral section of either the MLF or the ATD in order to reveal the relative influence of these two inputs. For this purpose, we have recorded in chronic alert cats the discharge of partially deafferented medial rectus motoneurons, simultaneously with eye movements. We were also interested in determining whether there was some type of recovery in motoneuronal firing with time following the selective lesion of each input, and in evaluating the possibility of compensatory mechanisms that could be developed by the pathway that was left intact. We demonstrate the functional and morphological prevalence of the MLF to drive motoneuronal firing and to compensate for the lesion of the ATD, likely through axonal sprouting. On the contrary, the ATD pathway was not able to compensate the more drastic effects of the MLF lesion.

MATERIALS AND METHODS

Experimental design and statistical analysis. Experiments were carried out in a total of 15 adult female cats weighing 2.5-3.5 kg, obtained from authorized breeders (University of Córdoba, Spain). Seven animals used for chronic recordings were divided into two groups to carry out the section of either the MLF (n = 3) or the ATD (n = 4). Four different animals were used for morphological analysis 3 days after ATD (n = 2) or MLF (n = 2) transection (namely, short-term). Four control animals were used for the anterograde tracing with biocytin from either the contralateral abducens (n = 2) or the ipsilateral lateral vestibular nucleus (n = 2). All experimental procedures were in compliance with the European Union Directive on the protection of animals used for scientific purposes (2010/63/EU), and the Spanish legislation (R.D. 55/2013).

JNeurosci Accepted Manuscript

Data were expressed as mean ± SEM. Comparison between electrophysiological and morphological data obtained from MLF- or ATD-sectioned animals, and controls, and at different times postlesion, were performed using the two-way ANOVA test, with an overall level of significance of 0.05, followed by *post hoc* comparisons using the Holm-Sidak test. All regression lines obtained in the present work were significant ($p < 0.05$). Statistics was performed with the aid of SigmaPlot software, version 11.0 (Systat Software, Inc., San Jose, CA, USA).

Procedures for chronic recordings. Animals were protected from vagal reflexes by means of atropine sulphate (0.5 mg/kg, i.m.), anesthetized with ketamine hydrochloride (20 mg/kg, i.m.) mixed with xylazine (0.5 mg/kg, i.m.) and then placed in a stereotaxic frame. Under aseptic conditions, stimulating electrodes, scleral coils and the recording chamber were implanted. For the antidromic identification of the oculomotor nucleus, silver bipolar electrodes were implanted in the IIIth nerve bilaterally. Additionally, a silver bipolar electrode was also implanted in the right VIth nerve at its exit from the brainstem for antidromic abducens nucleus identification. Two-turn Teflon-insulated stainless steel eye coils were implanted in the sclera of both eyes for eye movement recordings. Finally, two square-shaped windows were drilled in the skull to allow access both to the oculomotor nucleus in the midbrain, through the parietal cortex, and to the abducens nucleus in the pons, through the cerebellum. Acrylic chambers were built around the windows and bolted to the cranium for two purposes: first, to keep aseptic conditions, and second, as a part of a restraining system to prevent head movements during recordings. Animals were allowed to recover for 10-15 days. During this period, animal care was taken to ensure the healthy state of the animal.

Chronic recordings, analysis and lesion procedures. Recording sessions were carried out every two days except from the first week after axotomy, when recording

JNeurosci Accepted Manuscript

sessions occurred daily. During the recording sessions, animals were comfortably seated in a fabric bag, bandaged and placed in a Plexiglas box inside a coil frame, situated on a servo-controlled table to evoke the vestibulo-ocular reflex in cats. Eye movements were recorded using the magnetic field search-coil technique (Fuchs and Robinson, 1966).

Extracellular recordings in the medial rectus subdivision of the oculomotor nucleus were carried out with beveled glass micropipettes and filled with 2 M NaCl. Medial rectus subdivision of the oculomotor nucleus was located stereotaxically and with the aid of the antidromic field potential produced by electrical stimulation of the IIIrd nerve. Medial rectus motoneurons were identified by three different criteria: first, its preferential dorsolateral position in the nucleus; second, the increase in firing frequency during nasally-directed horizontal eye movements; third, the collision test between the antidromic and the orthodromic action potentials. The extracellular neuronal activity was amplified and filtered at a bandwidth of 10 Hz-10 kHz for display and digitalization purposes.

Eye and head movement and unitary neuronal recordings were stored for off-line analysis using a digitizing card (Power 1401, Cambridge Electronics Design). The range of eye movements was measured in controls and at different times postlesion, in both ATD- and MLF-sectioned animals, by selecting at least 21 periods of 100 s of spontaneous eye movements ($21 \leq n \leq 135$) for each lesion type and time point. The analysis of motoneuron firing rate was carried out following the protocol previously described (Davis-López de Carrizosa et al., 2009). Briefly, data of eye position (EP) and velocity (EV), head velocity (HV) and neuronal instantaneous firing rate (FR) were selected by means of custom-made programs written in Matlab 7.5. The firing rate of medial rectus motoneurons can be fitted according to the equation $FR = F_0 + k \cdot EP + r \cdot EV$, where the coefficients k (in spikes/s/degree) and r (in spikes/s/degree/s) are the

JNeurosci Accepted Manuscript

neuronal sensitivities to eye position (EP) and eye velocity (EV), respectively, and F_0 the ordinate intercept. During eye fixations, eye velocity is zero and, therefore, firing rate was fitted to the equation $FR = k \cdot EP + F_0$. Relationships between neuronal firing and EV (in degrees/second) during saccades were obtained by linear regression analysis after subtraction of the position component ($k \cdot EP$), which was calculated from the previously known sensitivity to eye position. During spontaneous eye movements, we named these two coefficients as k_s and r_s. Mean k_s and r_s values were obtained for each experimental group at every time point ($13 \leq n \leq 98$; n = number of cells recorded and analysed per group).

We also recorded eye and head position and velocity during the performance of the vestibulo-ocular reflex, elicited by rotating the table (and thus the animal's head) at known angles in the horizontal plane in darkness. We measured the gain of the reflex during a minimum of 20 intervals of 100 s ($20 \leq n \leq 51$) for each experimental group, and the velocity of the fast phases of the nystagmus for the different experimental situations ($42 \leq n \leq 339$; n = reflex hemicycles analysed for fast phases).

Motoneuron firing rate during vestibularly-induced eye movements also followed the above-described equation, but coefficients were named k_v and r_v. Moreover, we also analyzed separately the firing rate during on-directed and off-directed slow phases of the reflex. Mean values for k_v, k_v ON, k_v OFF, r_v, r_v ON and r_v OFF were calculated and compared statistically ($11 \leq n \leq 56$; n = number of cells analysed for each experimental group and time point). Due to the motor impairment of the eye ipsilateral to the fascicle transection, we used the eye movement of the contralateral eye for computations (de la Cruz et al., 2000). Recordings were carried out for a period of 2 months after lesion. Data were grouped in 0-5, 6-15, 16-25 days after lesion (namely,

JNeurosci Accepted Manuscript

200 short term -st-, 15, and 25 days after lesion, respectively) and between 25 days and 2
201 months after lesion (namely, long term, lt).

202 After an approximate recording period of two weeks in which control recordings
203 were carried out for each animal, the lesion was performed with a custom-made
204 microblade driven by a Camberra-type micromanipulator with an anteriorly directed
205 angle of 45 degrees to reach either the MLF or the ATD caudal to the trochlear nucleus.
206 The lesion tract was guided by stereotaxic coordinates and by the recordings of the
207 abducens nucleus and the MLF.

208 ***Retrograde medial rectus motoneuron labeling.*** Seven days before the end of
209 the experiment, medial rectus muscles were injected bilaterally with rhodamine
210 isothiocyanate (Sigma, St. Louis, MO, USA) for motoneuron retrograde identification.
211 Under general anesthesia and with the help of a dissecting microscope, the medial rectus
212 muscle of each eye was exposed and a volume of 8 µl of 20% rhodamine prepared in a
213 solution of 2% dimethylsulfoxide was injected using a Hamilton syringe.

214 ***Immunocytochemistry***. Animals were deeply anesthetized (sodium pentobarbital,
215 50 mg/kg, i.p.), and immediately perfused transcardially with saline followed by 4%
216 paraformaldehyde prepared in phosphate buffer 0.1 M, pH 7.4. Brainstem 50-µm-thick
217 coronal sections were obtained using a vibratome and collected in a solution of
218 phosphate buffered saline (PBS), pH 7.4, with 0.05% sodium azide for proper storage at
219 4 ºC. Selected sections were stained following the Nissl method to assess ATD and
220 MLF lesions.

221 To assess the presence of calretinin in vestibular neurons, as well as in the MLF
222 and ATD, and to check the correct localization of the lesion site, brainstem sections
223 were selected rostral to abducens and caudal to the trochlear nucleus. The proximal
224 stumps of sectioned axons were identified by immunocytochemistry against calretinin

JNeurosci Accepted Manuscript

(goat anti-calretinin, 1:2,500; AB1550; Chemicon, Temecula, CA, USA), a calcium-binding protein that is expressed by both abducens internuclear neurons and neurons located at the ventral portion of the lateral vestibular nucleus (de la Cruz et al., 1998; Highstein and Holstein, 2006). Briefly, tissue was blocked with 7% normal donkey serum (NDS) in PBS with 0.1% Triton X-100 (PBS-T) for 45 minutes, and incubated overnight at room temperature in a solution containing the primary antibody in PBS-T with 0.05% sodium azide and 3% NDS. After several washes, slices were incubated for 90 minutes in the secondary antibody (biotinylated donkey anti-goat IgG, Vector Laboratories, Burlingame, CA, USA, 1:500 in PBS-T). Sections were then rinsed and incubated for 90 minutes in the avidin-biotin-HRP complex (ABC, Vector Laboratories) prepared in PBS-T. After sequential washes in PBS, Tris-HCl buffered saline pH 7.4, Tris buffer 0.1 M pH 7.4 and Tris buffer 0.1 M pH 8, tissue was incubated in a solution of 0.05% 3,3'-diaminobenzidine tetrahydrochloride as the chromogen, 0.01% hydrogen peroxide and nickel sulphate 1 mM prepared in Tris buffer 0.1 M pH 8. Sections were thoroughly washed, mounted in glass slides and coversliped with DPX (Sigma). All animals showed the complete transection of the selected fascicle, either the MLF or the ATD.

In addition, we performed immunocytochemistry against different antibodies in midbrain sections obtained from animals sectioned at the ATD (n = 4 for the long-term, n = 2 for the short-term study) or at the MLF (n = 3 for the long-term, n = 2 for the short-term study). For the morphological study, long term was 2 months and short term was 3 days. First, to characterize the synaptic organization at the medial rectus motoneuron subdivision of the oculomotor nucleus, we used double immunofluorescence directed against calretinin, to evaluate MLF or ATD innervation, along with synaptophysin (mouse anti-Syn 1:2,000; MAB329; Millipore, Billerica, MA,

JNeurosci Accepted Manuscript

USA), a general marker of synaptic boutons. After several washes in PBS, midbrain sections were first incubated for 10 minutes in PBS with 1% sodium borohydride to increase antibody penetration, blocked as described above, and incubated for 12 hours at room temperature in a solution containing the primary antibody in PBS-T with 0.05% sodium azide and 3% NDS. After washing, sections were incubated for 2 hours in the secondary antibody, prepared in PBS-T (1:50; donkey anti-mouse IgG combined with fluorescein isothiocyanate -FITC- and donkey anti-goat IgG coupled to Cy5 for synaptophysin and calretinin visualization, respectively; Jackson Immunoresearch, West Grove, PA, USA). After rinsing, sections were mounted on glass slides and coverslipped with Vectashield (Vector Laboratories).

Second, we performed immunocytochemistry against GAP-43 (mouse anti-GAP-43, 1:1,000, MAB347, Millipore) to visualize axonal sprouting. Briefly, sections were blocked as described above, and incubated overnight at room temperature in PBS-T containing the primary antibody. After several rinses in PBS-T, sections were immersed in a solution containing the secondary antibody (1:50; donkey anti-mouse IgG combined with FITC; Jackson Immunoresearch).

Finally, some sections were selected to assess the possibility of changes in neurotrophin expression in partially deafferented medial rectus motoneurons. For this purpose, we performed immunocytochemistry against brain-derived neurotrophic factor (BDNF), neurotrophin-3 (NT-3) or nerve growth factor (NGF). Sections were incubated for 10 minutes in PBS with 1% sodium borohydride, blocked as described above, and incubated for 12 hours at room temperature in a solution containing the primary antibody in PBS-T with 0.05% sodium azide and 3% NDS (rabbit anti-BDNF sc-546, rabbit anti-NT3 sc-547 or rabbit anti-NGF sc-548, 1:100, Santa Cruz Biotechnology, Dallas, TX, USA). After several washes, sections were incubated first in the secondary

JNeurosci Accepted Manuscript

antibody (biotynilated donkey anti-rabbit 1:250, Vector Laboratories) for two hours, and then in streptavidin conjugated with Cy2 (1:800 in PBS, 45 minutes, Jackson ImmunoResearch).

Anterograde abducens/vestibular axon labeling. Four control animals were selected to track the course and final arborization of either abducens (n = 2) or vestibular (n = 2) axons towards medial rectus motoneurons. Briefly, biocytin (Sigma; 3% in Tris-HCl buffer 0.05 M, pH 7.4) was injected unilaterally using a micropipette, stereotaxically guided towards either the abducens nucleus or the lateral vestibular nucleus. Cathodal positive pulses of 7 μA and 80% duty cycle were applied for 15 minutes. Twenty four hours later, animals were deeply anesthetized (sodium pentobarbital, 50 mg/kg, i.p.) and perfused intracardially with physiological saline followed by the fixative containing 3% paraformaldehyde and 1.25% glutaraldehyde in 0.1 M sodium phosphate buffer, pH 7.4. Fifty μm-thick coronal sections were revealed using the ABC method (Vector Laboratories) prepared in PBS-T, and treated as described above to reveal the peroxidase reaction. Selected sections were counterstained with 0.5% toluidine blue for Nissl staining.

Image analysis. In the anterograde labeling experiments, brainstem sections were observed and images captured using a Zeiss optical conventional microscope connected to a camera (AXIOCAM ERc 5s) and a computer for image storage and analysis. Control sections were used to count the number of calretinin-positive axonal processes located inside the limits of the MLF or the ATD per slice. Media and standard error of the mean (SEM) were calculated to compare the extension of each projection on medial rectus motoneurons.

Midbrain immunostained sections were observed and images captured using a Zeiss LSM Duo confocal microscope (Zeiss, Oberkochen, Germany). Lasers DPSS 561

JNeurosci Accepted Manuscript

nm, argon 488 nm and HeNe 633 nm were used to excite rhodamine, FITC or Cy2, and Cy5, respectively. For the analysis of synaptic coverage around medial rectus motoneuron somata, images of single focal plane were made using the 63x oil immersion objective. Using ImageJ software (NIH), the number of axon terminals per soma was counted, and the somatic coverage was calculated as the percentage of the soma perimeter that was occupied by synaptophysin- or calretinin-immunoreactive boutons ($32 \leq n \leq 268$; n = number of cells analysed). For the analysis of synaptic density in the neuropil and GAP-43 expression, we used the oil immersion 40x objective. Random-selected squares of 30.5 x 30.5 μm through the neuropil were used to measure optical density. Background level was subtracted and the values of optical density were normalized with respect to the control side of the same section ($210 \leq n \leq 1300$; n = number of squares selected per experimental group and time point). For the analysis of neurotrophin expression, optical density was measured inside the cytoplasm of control and deafferented medial rectus motoneurons of the same section. After background level subtraction, data were expressed for each cell as the percentage with respect to the mean of the control values in the same section ($22 \leq n \leq 161$ for BDNF; $24 \leq n \leq 138$ for NT-3; $17 \leq n \leq 169$ for NGF; n = number of cells selected per experimental group and time point).

RESULTS

Comparison of abducens and vestibular inputs to medial rectus motoneurons

Anterograde transport of biocytin, injected either in the abducens nucleus or in the lateral vestibular nucleus (Fig. 1*A*,*B*, respectively, asterisks) of control animals, allowed the tracing of both neuronal afferences to medial rectus motoneurons. As previously described (Biefang, 1978), axons from abducens internuclear neurons cross

JNeurosci Accepted Manuscript

the midline at the level of the abducens nucleus and project rostrally through the contralateral MLF (Fig. 1*C*), a bundle of axons that course the brainstem longitudinally, in a dorso-medial position. Abducens projection onto medial rectus motoneurons was densely packed at the medial rectus subdivision of the oculomotor nucleus (Fig. 1*E*, arrows). On the other hand, as described by Baker and Highstein (1978), vestibular afferences to medial rectus motoneurons project through the ipsilateral ATD, a fascicle located immediately lateral to the MLF (Fig. 1*D*), and reach the oculomotor nucleus forming a much smaller and less branched terminal net of axons when compared with that of abducens internuclear neurons (Fig. 1*F*, arrows). Axonal quantification revealed a 4-fold higher number of labeled axons in the MLF than in the ATD (818.25 ± 26.82 and 243.25 ± 34.67 positive axons per section in MLF and ATD, respectively, mean ± SEM, $n = 4$, t-test; $t(6) = 13.11$; $p < 0.001$). Higher magnification images showed that abducens internuclear neuron and vestibular axon terminals formed bouton-like varicosities (Fig. 1*G*,*J*, respectively). However, most abducens internuclear neuron terminals were found intermingled in the neuropil of the oculomotor nucleus (Fig. 1*H*,*I*), while vestibular afferences were found more frequently contacting medial rectus motoneuron cell bodies (Fig. 1*K*,*L*), in accordance with Nguyen et al. (1999).

Vestibular projection to medial rectus motoneurons is immunopositive against calretinin

Previous immunocytochemistry studies have shown that cat abducens internuclear and vestibular neurons express the calcium-binding protein calretinin (de la Cruz et al., 1998; Baizer and Baker, 2005). However, a demonstration of the presence of calretinin-positive axons in the ATD is still lacking. Fig. 2*A* shows a coronal section through the pons, immunostained against calretinin. As expected, abducens internuclear

JNeurosci Accepted Manuscript

neurons were positive for calretinin staining (area surrounded by the dashed line), but also the medial vestibular nucleus, which projects to the abducens nucleus, and the lateral vestibular neurons in the area of origin of the ATD (inset in Fig. 2*A*). These results were in agreement with those obtained from more rostral sections, in which calretinin-positive axons were found both in the MLF and the ATD (Fig. 2*B*). In ATD-sectioned animals, positive axons were only visible in the MLF but not in the sectioned ATD (Fig. 2*C*). Similarly, in MLF-sectioned animals, the lack of calretinin demonstrated the extent of the lesion (Fig 2*E*; asterisk). Therefore, calretinin immunostaining allowed checking the correct location of lesions as further assessed by Nissl staining (Fig 2 *D*, *F*).

Changes in spontaneous eye movements after selective deafferentation

Control unlesioned cats perform eye movements with a high degree of conjugacy. However, lack of afferent stimulation onto medial rectus motoneurons induced motor deficits, present from the onset of lesion. More precisely, in the first 5 days after MLF transection, the eye ipsilateral to the lesion side was unable to cross towards the contralateral oculomotor hemifield (Fig. 3*C*). The lack of MLF input onto medial rectus motoneurons was devastating for the movement of the affected eye (Fig. 3*C*, blue trace). On the other hand, ATD lesion also affected the ipsilateral eye but to a lesser degree and duration (Fig. 3*A*, green trace). In the following days, there was a progressive recovery of motor function in both ATD and MLF animals, but this recovery was much more pronounced in the ATD-lesioned animals (Fig. 3*B*,*D*). Spontaneous convergent eye movements could be detected throughout the entire recording period after both types of lesion. Figures 3*E* and 3*F* illustrate the linear regression lines obtained after representing the horizontal movement of the right eye

JNeurosci Accepted Manuscript

versus the left eye in the different groups. The slope of these plots (that we termed "m") was close to 1 in control data (black line). Short-term post-ATD lesion showed a small reduction in the range of movements of the ipsilateral eye (Fig. 3*E*, light green line). Interestingly, in the long term, ATD lesion-induced deficits on spontaneous eye movements disappeared and the slope returned to values similar to control (Fig. 3*E*, dark green line). In MLF animals, short-term recordings showed a severe reduction in the range of movements in the affected eye, which can be appreciated as a reduction in the m value (Fig. 3*F*, light blue line). The amplitude of movements increased with time, but the affected eye never reached the normal range (Fig. 3*F*, dark blue line).

The statistical analysis revealed differences between both the two different transections and the time postlesion in the ipsilateral eye movements (two-way ANOVA test, F (2,3) = 4.65; $p < 0.001$; Holm-Sidak method for multiple comparisons). Thus, in the short term (less than 5 days postlesion), the range of movements decreased after partial deafferentation, but this decrease was statistically larger ($p < 0.001$) in MLF than in ATD animals (19.9 ± 0.9 degrees, 28.0 ± 1.0 degrees; $n = 27$ and $n = 41$, respectively, data expressed as mean ± SEM) when compared with controls (33.5 ± 0.4 degrees, $n = 135$; Fig. 3*G*). There was a progressive recovery in the range of movements of both groups, which was more pronounced in the case of ATD animals. Thus, in the long term (more than 25 days postlesion) there were no statistical differences between controls and ATD animals (31.6 ± 1.1 degrees, $n = 26$), while MLF animals still exhibited lower values in the range of movements when compared with controls and long-term ATD animals (26.0 ± 0.6 degrees; $n = 29$, $p < 0.001$ for both comparisons; Fig. 3*G*). The statistical analysis of the m value offered similar results (Fig. 3*H*). In control animals, the m value was 0.90 ± 0.01 ($n = 135$). During the first 5 days after lesion, this value dropped to statistically lower ($p < 0.001$) values as compared to control (0.70 ± 0.03 and

JNeurosci Accepted Manuscript

0.55 ± 0.03; n = 41 and n = 27, in ATD and MLF animals, respectively) that were lower in MLF than in ATD animals ($p < 0.001$). There was a progressive recovery and in the long term, ATD animals exhibited m values similar to those of controls (0.88 ± 0.02, n = 26), that were higher ($p < 0.001$) than those obtained in the short term and in MLF animals at long term (0.74 ± 0.03, n = 29). The effects of MLF section also improved in the long term with respect to short term, but the recovery was incomplete and m values were lower to those of controls at any time point (two-way ANOVA test, F (2,3) = 15.65; $p < 0.001$; Holm-Sidak method for multiple comparisons).

Altogether, these results showed that vestibular input deprivation had a transient effect on horizontal motor range. In contrast, the axotomy of abducens internuclear neuron had a more drastic effect, which, although improved with time, never reached normal values.

Partial deafferentation induces eye movement deficits during the vestibulo-ocular reflex

Sinusoidal head rotation in the horizontal plane (Fig. 3*I-L*, red lines represent the inverted head velocity) induced compensatory eye movements with approximately the same velocity but in the opposite direction (Fig. 3*I-L*, dashed black lines for control eye velocity, colored lines for the affected eye). These slow displacements were interspersed by fast phases, in the same direction as head rotation, which re-centered the eye in the orbit (Fig. 3*I-L*). Thus, when the head moved to the left, the compensatory movements were directed to the right and the fast phases to the left. Vestibular deafferentation (ATD lesion) of medial rectus motoneurons altered the performance of the vestibulo-ocular reflex. Thus, the gain of the reflex, i.e, the ratio of eye velocity during the slow phases to head velocity, was reduced in the affected eye immediately after lesion and

JNeurosci Accepted Manuscript

during the following five days (Fig. 3*I*, solid green line). Moreover, the velocity of fast phases was reduced both in the on and off directions of the hemicycles of slow phases (orange and red dots, respectively). After the initial alterations, eye movements progressively recovered and were qualitatively similar to control from 15 days after deafferentation onwards (Fig. 3*J*, solid green line).

On the contrary, MLF transection produced a larger and permanent reduction in both the amplitude of fast phase velocity and the gain of the reflex (Fig. 3*K,L*, solid blue lines).

Statistical analysis confirmed that partial input depletion induced a reduction in the gain of the reflex during the first 5 days after lesion, that was even lower in MLF animals (0.90 ± 0.02, 0.78 ± 0.03 and 0.52 ± 0.03; $n = 47$, $n = 27$ and $n = 20$, $p < 0.001$, for control, ATD and MLF lesion, respectively; Fig. 3*M*). ATD animals recovered normal values at longer time periods (0.90 ± 0.01 at long term; $n = 28$), but in the case of MLF animals, gain values improved with time but never reached those described during control eye movements (for the long term, the gain was 0.72 ± 0.01, $n = 26$, $p < 0.001$; two-way ANOVA test, $F(2,3) = 6.93$; $p < 0.001$; Holm-Sidak method for multiple comparisons; Fig. 3*M*).

Control mean peak eye velocity of on-directed saccades was 101.2 ± 2.2 degrees/s ($n = 106$). During vestibularly-induced eye movements, we will refer to on-saccades to those occurring during the on hemicycles of the slow phases, and off-saccades to those during the off hemicycles of the reflex (Fig. 3*N,O*). Partial deafferentation induced a reduction in the velocity of on-saccades in the short term, that was statistically lower in MLF than in ATD animals (33.8 ± 2.1 and 61.3 ± 1.5 degrees/s; $n = 50$ and $n = 245$, respectively, $p < 0.001$; Fig. 3*N*). In the case of ATD-sectioned animals, this value returned to normality from 15 days postlesion onwards,

JNeurosci Accepted Manuscript

and remained similar to control until the end of the experiments (99.8 ± 2.2 degrees/s, *n* = 127, for the interval 15-25 days). In the case of MLF-sectioned animals, this recovery was not complete, and mean amplitude in the long term (75.0 ± 2.0 degrees/s, *n* = 60) resulted higher than that obtained between 0 and 5 days post-surgery, but lower ($p < 0.001$) than control and ATD long-term data (two-way ANOVA test, $F(2,3) = 27.29$; $p < 0.001$; Holm-Sidak method for multiple comparisons; Fig. 3*N*). Data obtained during off-directed saccades offered similar results: in the short-term, there was a reduction ($p < 0.001$) in the amplitude of saccades that was more drastic for MLF animals when compared to ATD animals (96.7 ± 1.9, 74.2 ± 0.9 and 53.5 ± 3.5 degrees/s; *n* = 106, *n* = 245 and *n* = 50, for control, ATD and MLF, respectively; Fig. 3*O*). The effects of partial deafferentation were transitory, and long-term data were different ($p < 0.001$) from short-term data between the two types of lesion (94.7 ± 1.4 and 78.4 ± 2.3 degrees/s; *n* = 124 and *n* = 60, for ATD and MLF, respectively), although only ATD animals recovered the normal amplitude of off-directed saccades (two-way ANOVA test, $F(2,3) = 13.44$; $p < 0.001$; Holm-Sidak method for multiple comparisons; Fig. 3*O*).

Firing pattern of partially-deafferented medial rectus motoneurons during spontaneous eye movements

Medial rectus motoneurons exhibited a tonic-phasic firing pattern, which resembled that described for abducens motoneurons, as previously reported (de la Cruz et al., 1989). Thus, firing rate increased tonically with successive ipsilateral eye fixations towards more adducting positions. During adducting eye movements, medial rectus motoneurons fired bursts of action potentials whose amplitude was directly proportional to the velocity of the eye (Fig. 4*A*, asterisk), while abducting movements were related to decreases in firing rate (Fig. 4*A*, dots). The slope of the regression line

JNeurosci Accepted Manuscript

obtained after plotting firing rate *versus* eye position indicated the neuronal sensitivity to eye position, k_s (Fig. 4*E*, black line), and that obtained after plotting firing rate *versus* eye velocity was r_s, that represented the neuronal sensitivity to eye velocity (Fig. 4*G*, black line).

After both MLF and ATD lesion, the overall firing rate was reduced, bursts of spikes during on-directed saccades were less pronounced (Fig. 4*B*,*C*, asterisks) and off-directed saccades were associated to smaller decreases in neuronal firing, that, however, often implicated complete firing pauses (Fig. 4*B*,*C*, dots). Nevertheless, long-term experiments did not show any firing alteration in ATD-lesioned animals, with normal firing rates and a correct modulation of activity in relation to on- and off-directed saccades (Fig. 4*D*, asterisks and dots, respectively). This recovery was absent in MLF-lesioned animals throughout the entire span of the experiments (Fig. 4*B*).

Plots representing firing rate *versus* eye position (Fig. 4*E*) or velocity (Fig. 4*G*) showed higher slopes, and thus higher k_s and r_s, in control (black lines), and long-term ATD recordings (dark green line), when compared to short-term recordings (ATD, light green and MLF, light blue) and long-term MLF data (dark blue).

Mean control k_s value was 4.4 ± 0.1 sp/s/deg (n = 98; Fig. 4*F*). Partial deafferentation produced a reduction ($p < 0.001$) in this value for both types of lesion (2.8 ± 0.2 and 1.6 ± 0.2 sp/s/deg; n = 34 and n = 13, for ATD and MLF animals, respectively, in the short term), that was higher in the case of MLF animals ($p = 0.007$). There was a rapid recovery in k_s values in the case of ATD-deprived motoneurons (Fig. 4*F*). Thus, 15 days after ATD lesion, k_s value was 3.8 ± 0.2 sp/s/deg (n = 33), and remained unchanged in the long term (4.2 ± 0.3 sp/s/deg, n = 23, for data recorded >25 days after lesion). On the contrary, k_s values of MLF animals did not recover with time, and were lower than controls and ATD data for the same time point in any time selected

JNeurosci Accepted Manuscript

(2.8 ± 0.2 sp/s/deg; n = 21, $p < 0.001$, > 25 days after lesion; two-way ANOVA test, F (2,3) = 2.75; p = 0.012; Holm-Sidak method for multiple comparisons; Fig. 4*F*). Similar results were obtained for the analysis of r_s (Fig. 4*H*): mean control value (0.48 ± 0.02 sp/s/deg/s, n = 98) was reduced after both types of lesion in the short term (0.28 ± 0.02 sp/s/deg/s and 0.15 ± 0.02 sp/s/deg/s; n = 34 and n = 13, $p < 0.001$, for ATD and MLF groups, respectively). In the case of MLF animals, this value remained lower ($p <$ 0.001) than control for the whole experimental period (0.21 ± 0.02 sp/s/deg/s, n = 21, > 25 days after lesion). On the contrary, vestibular input depletion only produced short-term effects, that returned to normality from 15 days after lesion onwards (0.42 ± 0.03 sp/s/deg/s; n = 22, for the interval 15-25 days, two-way ANOVA test, F (2,3) = 3.10; p =0.005; Holm-Sidak method for multiple comparisons; Fig. 4*H*).

Therefore, k_s and r_s in medial rectus motoneurons decreased in the first 5 days ensuing ATD or MLF lesion, but recovered with time only after ATD section.

Synaptic input depletion impairs eye-related firing rate during the vestibulo-ocular reflex.

Figure 5A shows eye position and velocity, as well as related motoneuron firing rate, during the performance of the vestibulo-ocular reflex for a control cell. Eye velocity nearly overlaps with head velocity, so that the control gain was close to 1. Control motoneurons discharge closely resembled eye position, as seen during the slow phases of the reflex, with bursts or pauses of spikes during the on- or off-directed fast phases of the nystagmus, respectively. The modulation of motoneuron firing rate also changed after selective deafferentation during vestibularly-induced eye movements. In the short term, both ATD and MLF sections had similar effects on firing discharge: a reduction in the modulation related to both eye position and velocity (Fig. 5*C*). In

JNeurosci Accepted Manuscript

contrast, long-term recordings showed differences between these two groups. Thus, MLF animals produced similar results when compared to those obtained in the first days after lesion (Fig. 5*B*). However, cells recorded from 25 days onwards after ATD transection modulated their firing rate in relation to eye movements in a way that resembled that observed in the control situation (Fig. 5*D*). Plots of firing rate *versus* eye position or velocity were made to obtain the slopes of the regression lines, which are named neuronal sensitivity to eye position or to eye velocity during the vestibulo-ocular reflex (k_v or r_v, Fig. 5*E,I*, respectively). As expected, statistical analyses (two-way ANOVA test, F (2,3) = 2.32 and 2.72; p = 0.033 and 0.014 for k_v and r_v, respectively; Holm-Sidak method for multiple comparisons) showed a decrease in both k_v and r_v in the first 5 days after lesion (Fig. 5*F,J*, respectively,; k_v values of 5.1 ± 0.3, 2.7 ± 0.2 and 1.6 ± 0.3 sp/s/deg; r_v values of 0.72 ± 0.03, 0.43 ± 0.03 and 0.39 ± 0.07 sp/s/deg/s; n = 56, n = 23 and n = 11, $p < 0.001$, in control, ATD and MLF animals, respectively). This decrease remained throughout the time course of the experiments in the case of MLF-sectioned animals both for k_v and r_v (Fig. 5*F,J*, respectively). However, deprivation of vestibular input did not produce permanent changes, and data from 15 days pot-lesion onwards were similar to control (Fig. 5*F,J*).

To perform a more accurate analysis and reach a better comprehension of the role of abducens and vestibular inputs on medial rectus motoneurons, we analyzed separately neuronal sensitivity during on-directed and off-directed slow phases of the reflex. Again, the reduction in k_v and r_v values observed a few days after lesion during on- (k_v ON in Fig. 5*G*; r_v ON in Fig. 5*K;* two-way ANOVA test, F (2,3) = 2.16 and 2.39; p = 0.046 and 0.028 for k_v ON and r_v ON, respectively; Holm-Sidak method for multiple comparisons) and off-directed slow phases (k_v OFF in Fig. 5*H*; r_v OFF in Fig. 5*L;* two-way ANOVA test, F (2,3) = 2.22 and 2.36; p = 0.041 and 0.030 for k_v ON and r_v ON,

JNeurosci Accepted Manuscript

respectively; Holm-Sidak method for multiple comparisons) was permanent after abducens input depletion, but returned to normal values in ATD animals.

Reduction in synaptic coverage of medial rectus motoneurons after partial deafferentation

Partial deafferentation produced a reduction in both synaptophysin (Fig. 6*A*,*B*,*E*,*F*) and calretinin (Fig. 6*C*,*D*,*G*,*H*) staining in the neuropil around medial rectus motoneurons, measured as the percentage of optical density in relation to the control side (Fig. 6*I*,*J*). Statistical analysis revealed that this reduction was more drastic after MLF section when compared to ATD data at any time point (Fig. 6*K*,*L*) in accordance with previous reports pointing to a segregated innervation of medial rectus motoneurons (Nguyen et al., 1999). No differences were found between short- and long-term data, in ATD animals. However, MLF transection produced a decrease in both synaptophysin and calretinin staining that increased with time. Nevertheless, neither synaptophysin nor calretinin immunostaining in the neuropil yielded the control level in the long term after both types of lesion, although the reduction in MLF-sectioned animals was higher than in those animals with ATD section (Fig. 6*K*,*L*). Thus, in the long term, synaptophysin optical density in the neuropil was 57.0 ± 2.7% (n = 380 measurements) after MLF transection, which was significantly lower ($p < 0.01$) than after ATD lesion (84.8 ± 3.0%; n = 380), and in both cases synaptophysin optical density was lower than control (100 ± 1.7%, n = 1300, $p < 0.01$, two-way ANOVA test, $F(1,2) = 4.35$; $p = 0.013$; Holm-Sidak method for multiple comparisons).

MLF and ATD transection also produced a decrease in the synaptic coverage around cell bodies, measured as the percentage of the soma perimeter covered by synaptophysin- or calretinin-positive terminals, as shown in Fig. 7*A-E* (synaptophysin) and 7*F-J* (calretinin). Neither in the short nor in the long term we found changes in both

JNeurosci Accepted Manuscript

soma diameter or perimeter due to different lesions (Two-way ANOVA test, F(1,2) = 0.25; p = 0.779 for perimeter and F (1,2) = 1.179, p = 0.308; Holm-Sidak method for multiple comparisons; not illustrated). Thus, control motoneurons showed a large percentage of their soma surrounded by bouton-like processes stained against synaptophysin (Fig. 7*K*, 38.2 ± 0.5%, n = 268 cells). Calretinin staining allowed the specific labeling of abducens and vestibular innervation, which covered approximately a 29.0 ± 0.5% of the soma perimeter (Fig. 7*L*, n = 268). On the contrary, these terminal processes were scarcer after partial deafferentation at any time point and for both types of lesion. Thus, the percentage of soma perimeter covered by synaptophysin-immunopositive terminals was reduced after lesion (27.8 ± 0.8% and 33.4 ± 1.2%; n = 96 and n = 32; $p < 0.001$ and p = 0.001, for comparisons between controls and short-term ATD or MLF, respectively), and did not recover with time (32.2 ± 0.7%, 32.2 ± 0.9%; n = 101 and n = 71, $p < 0.001$, for long-term ATD and MLF, respectively; Fig 7*K*). Statistical analysis revealed that the higher reduction with respect to control ($p <$ 0.001) was that observed 3 days after ATD transection (Fig. 7*K*, ATD short term, ATDst), but this value increased two months after lesion (Fig. 7*K*, ATD long term, ATDlt; $p < 0.001$), suggesting a synaptic plastic process. MLF transection produced the less drastic reduction, that however did not improve with time (Fig. 7*K*; two-way ANOVA test; F (1,2) = 6.34; p = 0.002; Holm-Sidak method for multiple comparisons). These results are in agreement with previous research indicating a stronger vestibular innervation at the somatic level of medial rectus motoneurons when compared with abducens inputs (Nguyen et al., 1999). To assess whether changes in synaptic coverage were due to differences in the number of boutons contacting medial rectus motoneurons, we also counted and compared the number of synaptophysin-positive boutons around the soma perimeter (Fig. 7*M*). Results were consistent with synaptic coverage data:

JNeurosci Accepted Manuscript

ATD transection produced a more drastic reduction in the number of somatic boutons (18.2 ± 0.6, n = 96, short term), which was lower ($p < 0.001$) than control (25.5 ± 0.4, n = 268), but also lower than long-term ATD and short-term MLF data (21.0 ± 0.6, 22.1 ± 0.9, n = 101, n = 32; p = 0.002, p = 0.003, for long-term ATD and short-term MLF, respectively; two-way ANOVA test; F (1,2) = 4.18; p = 0.016; Holm-Sidak method for multiple comparisons). Interestingly, according to the present data, synaptic coverage in long-term ATD animals increased in relation to the short-term data, although it was still lower than control (Fig. 7 *K*,*M*). This result implies that after ATD transection, there must be a rapid degeneration of terminals around the soma (ATDst), but that 2 months after lesion (ATDlt) other new terminals covered the gaps left by the degenerated boutons, likely by axonal sprouting of intact MLF axons, which could explain the recovery in the motor function.

To determine changes in vestibular innervation after MLF transection, or abducens innervation after ATD lesion, we also stained axon terminals against calretinin. Results, both for synaptic coverage and number of boutons around cell bodies, were similar to those described for synaptophysin-stained terminals (Fig. 7*L*,*N*; two-way ANOVA test; F (1,2) = 3.21 and 3.68; p = 0.041 and 0.026 for synaptic coverage and number of boutons, respectively; Holm-Sidak method for multiple comparisons).

Induction of GAP-43 expression in medial rectus motoneuron inputs after partial deafferentation

To ascertain the possible molecular bases for this sprouting, we performed immunostaining against GAP-43, a protein that has been associated with axon growth.

JNeurosci Accepted Manuscript

Images of short-term animals showed an intense GAP-43 labeling after both ATD (Fig. 8*A*) and MLF (Fig. 8*C*) transections. However, images obtained in the long-term (Fig. 8*B*,*D* for ATD and MLF animals, respectively), showed a scarce staining, similar to that observed in the control side (Fig. 8*E*). Comparisons of optical density in the neuropil, normalized to the control side of the same section, confirmed qualitative observations: partial deafferentation produced an increased expression of GAP-43 in the remaining intact axons, which was more intense ($p < 0.001$) after ATD transection (336.1 ± 14.5%, $n = 258$ measurements) when compared to MLF (179.2 ± 8.0%, $n = 210$). However, two months after lesion, all values returned to normality (95.2 ± 4.9% and 110.9 ± 9.3%; $n = 286$ and $n = 145$ for ATD and MLF, respectively; 100 ± 3.3% for control, $n = 899$; two-way ANOVA test; $F(1,2) = 213.124$; $p < 0.001$; Holm-Sidak method for multiple comparisons; Fig. 8*F*). These results indicated that the synaptic remodelling found two months after lesion correlated well with an increase in GAP-43 expression, especially after ATD lesion. However, in the case of MLF animals, this change was not enough to induce an increase in medial rectus motoneuron inputs.

Increased neurotrophin expression in partially deafferented medial rectus motoneurons

Immunocytochemistry against BDNF, NT-3 and NGF was performed to elucidate the possible trophic mechanisms implicated in axon sprouting after partial deafferentation. Control medial rectus motoneurons resulted positive for the three neurotrophins (Fig. 9*A*-*C*). The three different antibodies produced a similar homogeneous labeling of motoneuronal somata.

Neurotrophins were also present in medial rectus motoneurons after selective deafferentation at any analyzed time point. However, images obtained in the short-term,

JNeurosci Accepted Manuscript

after both ATD (Fig. 9*D-F*) or MLF (Fig. 9*J-L*) transection, exhibited a more intense staining when compared to motoneurons present in the control side of the same section. Two months after lesion, however, immunostaining was weak and resembled that obtained in control cells (Fig. 9*G-I* for ATD animals and *M-O* for MLF animals).

Analysis of cytoplasmic optical density, expressed as percentages relative to the control side, offered similar results for BDNF (Fig. 9*P*), NT-3 (Fig. 9*Q*) or NGF (Fig. 9*R*). In the short term, there was a statistically significant increase in BDNF (114.6 ± 3.0% and 110.1 ± 2.0%; $22 \leq n \leq 161$; $p < 0.001$, for ATD and MLF, respectively), NT-3 (121.2 ± 4.9% and 117.8 ± 2.8%; $24 \leq n \leq 138$; $p < 0.001$, for ATD and MLF, respectively) and NGF (118.8 ± 4.2% and 110.1 ± 1.9%; $17 \leq n \leq 169$; $p < 0.001$, for ATD and MLF, respectively) with respect to controls (Fig. 9*P*-R, two-way ANOVA test; $F(1,2) = 9.69$, 7.16 and 6.76; $p < 0.001$, for BDNF, NT-3 and NGF, respectively; Holm-Sidak method for multiple comparisons). However, there were no differences in neurotrophin staining between long-term and control motoneurons, indicating a correlation between the increase of neurotrophin and GAP-43 labeling.

DISCUSSION

The present study compares for the first time the role of the two main pontine inputs to medial rectus motoneurons on their discharge characteristics by lesion experiments. MLF lesion produced more drastic and long-lasting changes in both eye movements and motoneuron firing rate than ATD section. On the other hand, long-term data pointed to a higher plastic capability of the MLF than the ATD. Plastic rearrangement of remaining inputs might be mediated by trophic factors, through the regulation of GAP-43 expression.

JNeurosci Accepted Manuscript

Short-term effects of selective medial rectus motoneuron deafferentation

Medial rectus motoneuron partial deafferentation involved a reduction in the motor range of the ipsilateral eye. This reduction was appreciated in ATD animals, but changes were more drastic after MLF section. As previously described (de la Cruz et al., 2000), cats with a transection of the MLF were not able to move the affected eye towards the "on" visual hemifield. Also, the maximum range was reduced. ATD transection produced similar deficits, but to a lesser extent. Alterations were also observed during vestibularly-induced eye movements. As described previously (de la Cruz y col., 2000), MLF section induced deficits in the amplitude of compensatory saccades and in the gain of the vestibulo-ocular reflex. ATD deprivation induced similar results but less pronounced than those after MLF transection, in spite of the vestibular origin of the ATD. A possible explanation for this result could be that the ATD projection is quantitatively smaller than that of the MLF (Baker and Highstein, 1978; Carpenter and Carleton, 1983, present data).

Partial deafferentation produced a decreased firing rate and a reduction in spontaneous and vestibular signals, which were comparable to those described for abducens internuclear and motoneurons after axotomy (Delgado-García et al., 1988c; de la Cruz et al., 2000; Davis-López de Carrizosa et al., 2009). In fact, axotomy leads to a retrograde synaptic stripping (Pastor et al., 2000), which implies a decrease in eye-related signals in abducens neurons (de la Cruz et al., 2000). Whereas axotomy produces a general afferent stripping, the selective removal by deafferentation results specific. However, given the similarity of physiological results with axotomy it should be concluded that the MLF input is crucial for the firing of medial rectus motoneurons and not replaceable by the ATD.

JNeurosci Accepted Manuscript

In the short term, the effects of ATD or MLF transection on motoneuron firing pattern were similar. In agreement with our results, ATD has been described as carrying not only head velocity information but also eye position signal (although weak) and, thus, the vestibular and MLF pathways would carry similar information, which might be considered as redundant (Furuya and Markham, 1981; Reisine et al., 1981). A different hypothesis points to an additive action of both inputs, so that both of them would be necessary to properly activate medial rectus motoneurons (Baker and Highstein, 1978). In addition, based on the different distribution of vestibular (somatic) and abducens (dendritic) terminals on medial rectus motoneurons (Nguyen et al., 1999), vestibular inputs have been suggested to play a role in the balance of motoneuron excitability, which would serve as a control gate for MLF signals. Our results confirmed MLF/ATD terminal distribution, and although motoneuron firing parameters decreased after both types of lesion, it should be emphasized that MLF lesion yielded more pronounced changes than ATD section, suggesting a more relevant role for the MLF pathway but, also, that ATD is not a functionally redundant pathway.

Long-term effects of ATD/MLF section on medial rectus motoneuron discharge properties and eye movements

Long-term recordings of eye movements and firing rate of medial rectus motoneurons after MLF section revealed absence of significant recovery with time. In contrast, ATD animals exhibited a complete recovery of eye movements, which was accompanied by an equally complete recovery in motoneuron discharge characteristics, during both spontaneous and vestibularly-induced eye movements. In order to understand the possible mechanisms mediating this recovery, we performed morphological analysis of medial rectus motoneuron innervation. As stated above,

JNeurosci Accepted Manuscript

Nguyen et al. (1999) postulated that ATD input to medial rectus motoneurons project mainly on somata and proximal dendrites, while MLF inputs innervate more profusely distal dendrites. Our results are in agreement with this hypothesis, since 1) we observed a higher decrease in neuropil innervation after MLF than after ATD transection, and 2) although we did not detect differences in synaptic coverage around soma between long-term ATD and MLF animals, by 3 days postlesion there was a larger reduction in somatic innervation after ATD than after MLF lesion. This result implies, on one hand, that indeed, ATD axons end preferentially on motoneuron somatic membrane, and on the other hand, that there must be a compensatory mechanism after ATD depletion that allows the replacement of lost synaptic inputs. This hypothesis would fit with motor and neurophysiological data.

Sprouting after partial deafferentation has been described previously (Lund and Lund, 1971; Matthews et al., 1976; Lee et al., 1977; Masliah et al., 1991; Bäurle et al., 1992; Zhang et al., 1995). In our experiments, the most likely source of sprouting axons arose from the abducens internuclear neurons. This assumption would correlate well with the observed increase in calretinin staining after long-term ATD section.

However, besides the formation of new terminals, it cannot be discarded that other plastic processes could have been involved in functional recovery, such as increased synaptic efficacy between abducens internuclear neurons and medial rectus motoneurons, as described in deafferented vestibular neurons (Him and Dutia, 2001).

The same compensatory mechanisms could take place after MLF transection. However, the effects of this type of lesion were permanent, since two months postlesion all firing parameters were lower than in control cells. We hypothesize that the ATD projection, with a few number of axons, is not sufficient to replace the information lost after the axotomy of the much larger projection of abducens internuclear neurons.

JNeurosci Accepted Manuscript

748 The severance of the MLF induces the internuclear ophthalmoplegia syndrome
749 without preventing vergence (Gamlin 1989b). The MLF comprises not only the
750 ascending abducens internuclear neurons but the descending oculomotor internuclear
751 neurons. As reported previously, neither the abducens internuclear neurons (Gamlin et
752 al., 1989a) nor the oculomotor internuclear neurons (Clendaniel and Mays, 1994) carry
753 appropriate signals for vergence. It is interesting to note that the severance of the
754 oculomotor internuclear neurons does not produce ophthalmoplegia of the contralateral
755 eye. Therefore, this projection should be comparably smaller than that of the abducens
756 internuclear neurons.

757 ATD neurons could support firing of medial rectus motoneurons during
758 convergence because they support an excitatory and ipsilateral projection to these
759 motoneurons. However, the eye position sensitivity of ATD neurons makes them
760 insufficient to support vergence (Reisine and Highstein, 1979). Other mesencephalic
761 neurons projecting to the oculomotor nucleus and carrying signals related to both
762 accommodation and/or vergence are the most appropriate neurons to ignite and sustain
763 the vergence circuit (Zhang et al., 1992).

764 **Possible molecular mechanisms for medial rectus motoneuron reinnervation**

765 Axonal sprouting is accompanied by an increase in GAP-43, a growth-associated
766 protein whose expression is increased during axon elongation (Lynch et al., 1976;
767 Benowitz et al., 1990; Lin et al., 1992; Gomez-Pinilla et al., 2004). The present results
768 showed an increase in GAP-43 in the neuropil of medial rectus motoneuron subdivision
769 three days after partial deafferentation, a period in which the physiological properties of
770 the affected motoneurons were still altered. However, two months postlesion, GAP-43
771 levels were similar to those of the control side, in coincidence with partial (MLF) or
772 complete (ATD) recovery. We postulate that, in the short term, remaining axons might

JNeurosci Accepted Manuscript

be elongating their terminals covering the gaps left by lesion, but new synapses would have not been established yet, in accordance to physiological results. However, in the long term, synapses would be already functional and GAP-43 down-regulated, which would explain the recovery in motoneuron function (Fig. 10).

The molecular mechanisms by which GAP-43 was elevated in response to partial deafferentation could be linked to the increase in neurotrophin content in medial rectus motoneurons. In fact, exogenous NGF and NT-3 have been proven to increase sprouting after partial deafferentation in spinal cord motoneurons (Scott et al., 2005), and BDNF administration induces sprouting of spinal axons after spinal cord crush (Jakeman et al., 1988). Moreover, it has been proposed that NGF, BDNF and NT-3 regulate GAP-43 content in growing axons (Perrone-Pizzozero et al., 1991, 1993, Mohiuddin et al., 1995; Federoff et al., 1998; Dinocourt et al., 2006; Geremia et al., 2010; Sanna et al., 2017) and that BDNF and NT-3 increase in spinal motoneurons after partial deafferentation (Johnson et al., 2000). Thus, considering that, first, the motoneuronal neurotrophin content was higher three days after partial deafferentation, and second, that both abducens internuclear and lateral vestibular neurons express the high affinity neurotrophin receptors (Benitez-Temiño et al., 2004), it could be possible that neurotrophins released by motoneurons would be causally related to GAP-43-mediated sprouting (Fig. 10).

In summary, the major difference found between ATD and MLF lesion was the long-term complete recovery occurring after ATD transection, which was not present after MLF section, and that could be explained by regrowing of intact axons likely from abducens internuclear neurons.

JNeurosci Accepted Manuscript

REFERENCES

Baker R, Highstein SM (1978) Vestibular projections to medial rectus subdivision of oculomotor nucleus. J Neurophysiol 41: 1629-1646.

Baizer JS, Baker JF (2005) Immunoreactivity for calcium-binding proteins defines subregions of the vestibular nuclear complex of the cat. Exp Brain Res 164: 78-91.

Bäurle J, Gorver BG, Grüsser-Cornehls U (1992) Plasticity of GABAergic terminals in Deiters' nucleus of weaver mutant and normal mice: a quantitative light microscope study. Brain Res 591: 305-318.

Benítez-Temiño B, Morcuende S, Mentis GZ, de la Cruz RR, Pastor AM (2004) Expression of Trk receptors in the oculomotor system of the adult cat. J Comp Neurol. 473: 538-552.

Benowitz LI, Rodriguez WR, Neve RL (1990) The pattern of GAP-43 immunostaining changes in the rat hippocampal formation during reactive synaptogenesis. Brain Res Mol Brain Res 8: 17-23.

Biefang DC (1978) The course of direct projections from the abducens nucleus to the contralateral medial rectus subdivision of the oculomotor nucleus in the cat. Brain Res 145: 277-289.

Büttner-Ennever JA (2006) The extraocular motor nuclei: organization and functional neuroanatomy. In: Neuroanatomy of the Oculomotor System, Progress in Brain Research, vol. 151 (Büttner-Ennever JA, ed) pp. 95-126. Amsterdam: Elsevier.

Carpenter MB, Carleton SC (1983) Comparison of vestibular and abducens internuclear projections to the medial rectus subdivision of the oculomotor nucleus in the monkey. Brain Res 274: 144-149.

JNeurosci Accepted Manuscript

821 Carpenter MB, McMasters RE (1963) Disturbances of conjugate horizontal eye
822 movements in the monkey. II. Physiological effects and anatomical degeneration
823 resulting from lesions in the medial longitudinal fasciculus. Arch Neurol 8: 17-38.
824 Clendaniel RA, Mays LE (1994) Characteristics of antidromically identified oculomotor
825 internuclear neurons during vergence and versional eye movements. J Neurophysiol
826 71:1111-1127.
827 Davis-López de Carrizosa MA, Morado-Díaz CJ, Tena JJ, Benítez-Temiño B, Pecero
828 ML, Morcuende SR, de la Cruz RR, Pastor AM (2009) Complementary actions of
829 BDNF and neurotrophin-3 on the firing patterns and synaptic composition of
830 motoneurons. J Neurosci 29: 575-587.
831 de la Cruz RR, Delgado-García JM, Pastor AM (2000) Discharge characteristics of
832 axotomized abducens internuclear neurons in the adult cat. J Comp Neurol 427: 391-
833 404.
834 de la Cruz RR, Escudero M, Delgado-García JM (1989) Behaviour of medial rectus
835 motoneurons in the alert cat. Eur J Neurosci 1: 288-295.
836 de la Cruz RR, Pastor AM, Martínez-Guijarro FJ, López-García C, Delgado-García JM
837 (1998) Localization of parvalbumin, calretinin, and calbindin D-28k in identified
838 extraocular motoneurons and internuclear neurons of the cat. J Comp Neurol 390: 377-
839 391.
840 Delgado-García JM, del Pozo F, Baker R (1988a) Behavior of neurons in the abducens
841 nucleus of the alert cat- I. Motoneurons. Neuroscience 17: 929-952.
842 Delgado-García JM, del Pozo F, Baker R (1988b) Behavior of neurons in the abducens
843 nucleus of the alert cat- II. Internuclear neurons. Neuroscience 17: 953-973.

JNeurosci Accepted Manuscript

844 Delgado-García JM, del Pozo F, Spencer RF, Baker R (1988c) Behavior of neurons in
845 the abducens nucleus of the alert cat- III. Axotomized motoneurons. Neuroscience 24:
846 143-60.
847 Dinocourt C, Gallagher SE, Thompson SM (2006) Injury-induced axonal prouting in
848 the hippocampus is initiated by activation of trkB receptors. Eur J Neurosci 24: 1857-
849 1866.
850 Escudero M, Delgado-García JM (1988) Behavior of reticular, vestibular and prepositus
851 neurons terminating in the abducens nucleus of the alert cat. Exp Brain Res 71: 218-
852 222.
853 Federoff HJ, Grabczyk E, Fishman MC (1988) Dual regulation of GAP-43 gene
854 expression by nerve growth factor and glucocorticoids. J Biol Biochem 263: 19290-
855 19295.
856 Fuchs AF, Robinson DA (1966) A method for measuring horizontal and vertical eye
857 movement chronically in the monkey. J Appl Physiol 21: 1068-1070.
858 Fuchs AF, Scudder CA, Kaneko CRS (1988) Discharge patterns and recruitment order
859 of identified motoneurons and internuclear neurons in the monkey abducens nucleus. J
860 Neurophysiol 60: 1874-1895.
861 Furuya N, Markham CH (1981) Arborization of axons in oculomotor nucleus identified
862 by vestibular stimulation and intra-axonal injection of horseradish peroxidase. Exp
863 Brain Res 43: 289-303.
864 Gamlin PD, Gnadt JW, Mays LE (1989a) Abducens internuclear neurons carry an
865 inappropriate signal for ocular convergence. J Neurophysiol 62:70-81.
866 Gamlin PD, Gnadt JW, Mays LE (1989b) Lidocaine-induced unilateral internuclear
867 ophthalmoplegia: effects on convergence and conjugate eye movements. J Neurophysiol
868 62:82-95.

JNeurosci Accepted Manuscript

869 Geremia NM, Pettersson LME, Hasmatali JC, Hryciw T, Danielsen N, Schreyer DJ,
870 Valerie MK, Verge A (2010) Endogenous BDNF regulates induction of intrinsic
871 neuronal growth programs in injured sensory neurons. Exp Neurol 223: 128-142.
872 Gomez-Pinilla F, Ying Z, Roy RR, Hodgson J, Edgerton VR (2004) Afferent input
873 modulates neurotrophins and synaptic plasticity in the spinal cord. J Neurophysiol 92:
874 3423-3432.
875 González-Forero D, Morcuende S, Alvarez FJ, de la Cruz RR and Pastor AM (2005)
876 Transynaptic effects of tetanus neutoxin in the oculomotor system. Brain 128: 2175-
877 2188.
878 Grantyn R, Baker R, Grantyn A (1980) Morphological and physiological identification
879 of excitatory pontine reticular neurons projecting to the cat abducens nucleus and spinal
880 cord. Brain Res. 198: 221-228.
881 Highstein SM (1977) Abducens to medial rectus pathway in the MLF: a possible
882 cellular basis for the syndrome of internuclear ophthalmoplegia. In: Eye movements
883 (Brooks BA, Bajandas FJ, eds) pp. 127-143. New York: Plenum Publishing
884 Corporation.
885 Highstein SM, Baker R (1978) Excitatory termination of abducens internuclear neurons
886 on medial rectus motoneurons: relationship to syndrome of internuclear
887 ophthalmoplegia. J Neurophysiol 41: 1647-1661.
888 Highstein SM, Holstein GR (2006) The anatomy of the vestibular nuclei. Progress in
889 Brain Research, vol. 151 (Büttner-Ennever JA, ed) pp. 157-203. Amsterdam: Elsevier.
890 Hikosaka O, Igusa Y, Nakao S, Shimazu H (1978) Direct inhibitory synaptic linkage of
891 pontomedullary reticular burst neurons with abducens motoneurons in the cat. Exp
892 Brain Res 33: 337-352.

JNeurosci Accepted Manuscript

893 Him A, Dutia MB (2001) Intrinsic excitability changes in vestibular nucleus neurons
894 after unilateral deafferentation. Brain Res 908: 58-66.
895 Igusa A, Sasaki S, Shimazu H (1980) Excitatory premotor burst neurons in the cat
896 pontine reticular formation related to the quick phase of vestibular nystagmus. Brain
897 Res 182: 451-456.
898 Jakeman LB, Wei P, Guan Z, Stokes BT (1998) Brain-derived neurotrophic factor
899 stimulates hindlimb stepping and sprouting of cholinergic fibers after spinal cord injury.
900 Exp Neurol 154: 170-184.
901 Johnson RA, Okragly AJ, Haak-Frendscho M, Mitchell GS (2000) Cervical dorsal
902 rhizotomy increases brain-derived neurotrophic factor and neurotrophin-3 expression in
903 the ventral spinal cord. J Neurosci 20 RC77 (1-5).
904 Lee KS, Stanford EJ, Cotman CW, Lynch GS (1977) Ultrastructural evidence for
905 bouton proliferation in the partially deafferented dentate gyrus of the adult rat. Exp
906 Brain Res 29: 475-485.
907 Lin LH, Bock S, Carpenter K, Rose M, Norden JJ (1992) Synthesis and transport
908 of GAP-43 in entorhinal cortex neurons and perforant pathway during lesion-induced
909 sprouting and reactive synaptogenesis. Brain Res Mol Brain Res 14: 147-53.
910 Lund RD, Lund JS (1971) Modifications of synaptic patterns in the superior colliculus
911 of the rat during development and following deafferentation. Vision Res Suppl 3: 281-
912 298.
913 Lynch G, Gall C, Rose G, Cotman C (1976) Changes in the distribution of the dentate
914 gyrus associational system following unilateral or bilateral entorhinal lesions in the
915 adult rat. Brain Res 110: 57-71.

JNeurosci Accepted Manuscript

916 Masliah E, Fagan AM, Terry RD, DeTeresa R, Mallory M, Gage FH. (1991) Reactive
917 synaptogenesis assessed by synaptophysin immunoreactivity is associated with GAP-43
918 in the dentate gyrus of the adult rat. Exp Neurol 113: 131-142.

919 Matthews DA, Cotman C, Lynch G (1976) An electron microscopic study of lesion-
920 induced synaptogenesis in the dentate gyrus of the adult rat. II. Reappearance of
921 morphologically normal synaptic contacts. Brain Res 115: 23-41.

922 McCrea RA, Baker R (1985) Anatomical connections of the nucleus prepositus of the
923 cat. J Comp Neurol 237: 377-407.

924 McCrea RA, Strassman A, Highstein SM (1986) Morphology and physiology of
925 abducens motoneurons and internuclear neurons intracellularly injected with
926 horseradish peroxidase in alert squirrel monkeys. J Comp Neurol 243: 291-308.

927 McCrea RA, Yoshida K, Berthoz A, Baker R (1980) Eye movement related activity and
928 morphology of second order vestibular neurons terminating in the cat abducens nucleus.
929 Exp Brain Res 40: 468-473.

930 Mohiuddin L, Fernandez K, Tomlinson DR, Fernyhough P (1995) Nerve growth factor
931 and neurotrophin-3 enhance neurite outgrowth and up-regulate the levels of messenger
932 RNA for growth-associated protein GAP-43 and Tal a-tubulin in cultured adult rat
933 sensory neurons. Neuroscience Letters 185: 20-23.

934 Nguyen LT, Baker R, Spencer RF (1999) Abducens internuclear and ascending tract of
935 Deiters inputs to medial rectus motoneurons in the cat oculomotor nucleus: synaptic
936 organization. J Comp Neurol 405: 141-159.

937 Pastor AM, Delgado-García JM, Martínez-Guijarro FJ, López-García C, de la Cruz RR
938 (2000) Response of abducens internuclear neurons to axotomy in the adult cat. J Comp
939 Neurol 427: 370-390.

JNeurosci Accepted Manuscript

940 Pastor AM, Torres B, Delgado-García JM, Baker R (1991) Discharge characteristics of
941 medial rectus and abducens motoneurons in the goldfish. J Neurophysiol 66: 2125-
942 2140.
943 Perrone-Bizzozero NI, Neve RL, Irwin N, Lewis S, Fischer I, Benowitz LI (1991) Post-
944 transcriptional regulation of GAP-43 mRNA levels during neuronal differentiation and
945 nerve regeneration. Mol Cell Neurosci 2: 402-409.
946 Perrone-Bizzozero NI**,** Cansino VV, Kohn DT (1993) Posttranscriptional regulation of
947 GAP-43 gene expression in PC12 cells through protein kinase C-dependent stabilization
948 of the mRNA J Cell Biol 120: 1263-1270.
949 Reisine H, Highstein SM (1979) The ascending tract of Deiters´ conveys a head
950 velocity signal to medial rectus motoneurons. Brain Res 170: 172-176.
951 Reisine H, Strassman A, Highstein SM (1981) Eye position and eye velocity signals are
952 conveyed to medial rectus motoneurons in the alert cat by the ascending tract of
953 Deiters´. Brain Res 211: 153-157.
954 Sanna MD, Ghelardini C, Galeotti N (2017) HuD-mediated distinct BDNF regulatory
955 pathways promote regeneration after nerve injury. Brain Res 1659: 55-63.
956 Scott ALM, Borisoff JF, Ramer MS (2005) Deafferentation and neurotrophin-mediated
957 intraspinal sprouting: a central role for the p75 neurotrophin receptor. Eur J Neurosci
958 21: 81-92.
959 Zhang B, Goldberger ME, Wu LF, Murray M (1995) Plasticity of complex terminals in
960 lamina II in partially deafferented spinal cord: the cat spared root preparation. Exp
961 Neurol 132: 186-193.
962 Zhang Y, Mays LE, Gamlin PDR (1992) Characteristics of near response cells
963 projecting to the oculomotor nucleus. J Neurophysiol 67:944-960.
964

JNeurosci Accepted Manuscript

965 **Figure legends**

966 **Figure 1.** Anterograde tracing of pontine medial rectus motoneuron afferences. ***A, B***,
967 Biocytin injection (asterisks) in the abducens (***A***) or lateral vestibular nuclei (***B***). VIIg:
968 genu of the facial nerve. The dashed line marks the approximate boundaries of the
969 abducens nucleus. ***C, D,*** Biocytin-labeled axons coursing through the contralateral MLF
970 (***C***, for the injection shown in ***A***) or the ipsilateral ATD (***D***, for the injection shown in
971 ***B***). Inset in ***D*** shows an enlarged image of the squared box in the ATD. ***E, F,*** Stained
972 axon terminals from abducens internuclear (***E***) or vestibular (***F***) neurons. Arrows show
973 the location of medial rectus subdivision. Vertical lines indicate the midline. ***G-L***,
974 Higher magnification images obtained from the same areas delimited by arrows in ***E***
975 (***G-I***) and ***F*** (***J-L***) showing biocytin-labeled terminals around the motoneurons. Scale
976 bars: 500 μm (in ***B*** for ***A*** and ***B***; in ***D*** for ***C*** and ***D***; in ***F*** for ***E*** and ***F***); 100 μm (***G*** and ***J***);
977 20 μm (in ***I*** for ***H*** and ***I***; in ***L*** for ***K*** and ***L***). Inset scale bar: 100 μm.
978
979 **Figure 2.** Lesion assessment using anti-calretinin immunostaining and Nissl labeling. ***A***,
980 Calretinin immunolabeled both abducens internuclear neurons (dashed line) and lateral
981 vestibular neurons (square). Inset shows a higher magnification image of the area
982 delimited by the square. VIIg: facial nerve genu. ***B,*** Calretinin-stained axons in both
983 control ATD and MLF tracts. Inset magnifies the square-delimited area. ***C,*** Lesion site
984 of the ATD demonstrated by the absence of calretinin and the presence of refringent
985 scar tissue under Nomarski transillumination (dashed lines delimiting area). ***D,*** Nissl
986 demonstration of the scar tissue (delimited by arrows) corresponding to the lateral span
987 of the ATD transection that spared the MLF (circled). ***E,*** Calretinin-stained section
988 rostral to the lesion site demonstrating lack of immunostaining (asterisk) in the severed
989 MLF. Calretinin-stained axons were present in the ATD (arrowheads). ***F,*** Nissl

JNeurosci Accepted Manuscript

990 demonstration of the unilateral lesion of the MLF (delineated by dashed line). Midline
991 is indicated by vertical dashed lines in ***D-F***. Scale bars: 500 μm in ***A, D*** and ***F***; 250 μm
992 in ***E*** stands for ***B, C*** and ***E***. Inset scale bars: 50 μm (in ***A***; in ***B*** for ***B*** and ***C***).
993
994 **Figure 3.** Changes in eye movements in response to MLF or ATD section. ***A-D,***
995 Spontaneous eye movements 2 days (***A***, ***C***) or 26 days (***B***, ***D***) after ATD (***A***, ***B***) or MLF
996 (***C***, ***D***) lesion. Solid lines correspond to the affected eye, while dashed lines illustrate the
997 control eye. Upwards deflections of eye position (EP, in degrees) indicate eye
998 movements to the left (L; R, to the right). ***E, F,*** Linear regression lines between
999 horizontal movement of both eyes, in either ATD (***E***) or MLF (***F***) lesioned animals. The
1000 slope of the regression lines (m) was used as an index of conjugacy. ***G, H,*** Time course
1001 of the range of eye movements (***G***) or the slope m (***H***) after selective deafferentation (21
1002 $\leq n \leq$ 135 intervals of 100 s of spontaneous eye movements). ***I-L,*** Vestibularly-induced
1003 eye velocity (EV, in degrees/s) 1 day (***I***, ***K***) or 26 days (***J***, ***L***) after ATD (***I***, ***J***) or MLF
1004 (***K***, ***L***) lesion. Head velocity is shown inverted in red for visual comparison with EV.
1005 Recordings of the affected eye are represented by colored solid lines and the control eye
1006 velocity is represented by black dashed lines. Note the reduction in the velocity of the
1007 fast phases of the reflex in the first five days after lesion, which returns to normal in
1008 ATD but not in MLF animals. Red and orange dots point to reductions in saccades
1009 occurring during the off- or on-hemicycles of the slow phases of the vestibulo-ocular
1010 reflex, respectively. ***M,*** Changes in the gain of the vestibulo-ocular reflex (VOR) with
1011 time, expressed as the ratio between eye and head velocity. ($20 \leq n \leq 51$ intervals of 100
1012 s of VOR analysed). ***N, O***, Two-way ANOVA comparisons of the effect of MLF or
1013 ATD sections at different time points (short term, 5 days postlesion; long term, more
1014 than 25 days postlesion) on the peak velocity of saccades (Sacc.') occurring during the

JNeurosci Accepted Manuscript

on hemicycles (hc.) of the slow phases of the VOR (***N***) or during the off slow phases (***O***, Sacc.' hc. OFF) ($42 \leq n \leq 339$ VOR hemicycles analysed for saccades). For ***M-O***, blue and green lines correspond to data from MLF and ATD animals, respectively. Control, black dot; short-term recordings, light-colored lines; long-term recordings, dark-colored lines. * indicates differences with controls. ● indicates differences with respect to short-term values within the same lesion type. # indicates differences between the two lesions at the same time point. Data are shown as mean ± SEM; st: short-term; lt: long-term; Two-way ANOVA, Holm-Sidak test, $p < 0.05$.

Figure 4. Effects of deafferentation on medial rectus motoneuron firing pattern during spontaneous eye movements. ***A-D,*** From top to bottom, horizontal right eye position (EP) and velocity (EV) and instantaneous firing rate (FR, in spikes/s) in a control animal (***A***), 30 days after MLF section (***B***), and either 2 or 39 days after ATD transection (***C*** and ***D***, respectively). L and R indicate movements towards the left and right, respectively. Asterisks indicate the occurrence of on-directed saccades and the associated bursts in neuronal firing (note the reduced bursts in ***B*** and ***C*** but not in ***D***). Dots point to off-directed saccades, related to decreases in firing rate. ***E-H,*** Correlation between firing rate and either horizontal eye position (EP, ***E***) or velocity (EV, ***G***). The slope of the linear regression lines is the neuronal sensitivity to eye position (k_s in ***E***) or velocity (r_s in ***G***). Note a short-term (st) decrease in k_s and r_s values after both types of lesion, which in the case of ATD animals returns to control in the long term (lt). Mean and SEM for k_s and r_s values were calculated and compared (***F*** and ***H***, respectively). Color codes are indicated in the figure. For ***F***, ***H***, * indicates differences with controls. ● indicates differences with respect to short-term values. # indicates differences between lesion groups at the same time point. Two-way ANOVA, Holm-Sidak test, $p <$

JNeurosci Accepted Manuscript

0.05; The number of cells analysed at each time point was 98 control cells, 34, 33, 22 and 23 for st, between 6 and 15, between 16 and 25 days and lt in ATD animals respectively, and 13, 31, 18 and 21 cells for MLF animals at the same time points, respectively. Same cells analysed for ***F***, ***H***.

Figure 5. Changes in firing pattern during vestibularly-induced eye movements. ***A-D***, From top to bottom: horizontal eye position (EP) and velocity (EV), and firing rate (FR) in a control animal (***A***), 30 days after MLF transection (***B***), and 3 or 44 days after ATD lesion (***C*** and ***D***, respectively). Inverted head velocity is indicated in middle plots by a red line. ***E, I***, Neuronal sensitivities to eye position (k_v, ***E***) and velocity (r_v, ***I***) calculated as the slope of the regression line obtained after plotting FR versus EP or EV, respectively. ***F-H,*** Time course of k_v values (***F***), and k_v values during on-directed (***G***) or off-directed slow phases of the VOR (***H***). ***J-L,*** Time course of r_v values (***J***), and r_v values during on-directed (***K***) or off-directed slow phases of the reflex (***L***). Color codes are indicated in the figure. For ***F-H*** and ***J-L***, * indicates differences with controls. ● indicates differences with short-term data within the same lesion type. # indicates differences between lesion types at the same time point. Data are shown as mean ± SEM. Two-way ANOVA, Holm-Sidak test, $p < 0.05$; the number of cells was 56 in the control situation, 23, 24, 19 and 20 in ATD animals and 11, 12, 11 and 13 cells in MLF animals at st, between 6 and 15, between 16 and 25 days and lt, respectively. Same cells analysed in ***F-H*** and ***J-L***.

Figure 6. Synaptic coverage in the neuropil measured as optical density. ***A-H,*** Confocal images of the medial rectus motoneuron subdivision, identified by retrograde rhodamine staining, in red, illustrating the presence of synaptophysin-positive terminals (***A***, ***B***, ***E***,

JNeurosci Accepted Manuscript

F; SYN, in green) and calretinin-positive axons (***C***, ***D***, ***G***, ***H***; CR, pseudocolored in white) in ATD (***A***-***D***) and MLF (***E***-***H***) animals. ***I, J,*** Images obtained from the control side. ***K, L,*** Comparisons of optical density (normalized to control values) at the neuropil of the nucleus in sections stained against synaptophysin (***K***) or calretinin (***L***); st: short-term; lt: long-term. For ***K***, ***L***, * indicates differences between the marked groups. ● indicates differences with short-term data within the same lesion type. # indicates differences between lesion types at the same time point; $210 \leq n \leq 1300$ measurements of optical density (same for ***K***, ***L*** in the double immunofluorescence). Two-way ANOVA, Holm-Sidak test, $p < 0.05$. Scale bar: 100 µm in ***J*** for ***A***-***J***.

Figure 7. Synaptic coverage of medial rectus motoneuron somata after selective partial deafferentation. ***A-E,*** Confocal microscope images of medial rectus motoneurons (labeled with rhodamine, in red) and synaptophysin-immunoreactive terminals (SYN, in green) surrounding neuron cell bodies in control (***A***), short-term ATD (***B***), long-term ATD (***C***), short-term MLF (***D***) and long-term MLF (***E***) animals. ***F-J,*** Same as above but for calretinin-immunoreactive terminals (CR, pseudocolored in white). ***K, M,*** Bar charts comparing mean ± SEM values of the synaptic coverage around soma perimeter (***K***), and number of boutons (***M***) in control (black bar), short-term ATD (light green), long-term ATD (dark green), short-term MLF (light blue) and long-term MLF (dark blue) groups using immunostaining against synaptophysin (SYN). ***L, N,*** Same as ***K***, ***M***, but for terminals stained against CR. For ***K-N***, *, # and ● indicate differences with controls, between lesions at the same time point, or between time points in the same lesion group, respectively. Two-way ANOVA, Holm-Sidak test, $p < 0.05$; $32 \leq n \leq 268$ cells. Same cells analysed for ***K-N***. Scale bar: 25 µm in ***J*** for ***A***-***J***.

JNeurosci Accepted Manuscript

Figure 8. Increased GAP-43 expression in short-term deafferentation. ***A-E,*** Confocal images illustrating changes in GAP-43 expression (in green) in the medial rectus motoneuron subdivision of the oculomotor nucleus (motoneurons identified by rhodamine staining in red) in ATD (***A***, ***B***) and MLF (***C***, ***D***) animals, at short-term (ST, ***A***, ***C***) and long-term (LT, ***B***, ***D***) periods, and in the control situation (***E***). Note the higher staining in short-term images compared with the other groups. ***F,*** Bar chart illustrating mean ± SEM optical density measured in the neuropil of control (black bar), short-term ATD (light green), long-term ATD (dark green), short-term MLF (light blue) and long-term MLF (dark blue) animals. Data were normalized with respect to control; $145 \leq n \leq 899$ measurements of optical density. *, # and ● indicate differences with control, between lesions at the same time point, or between time points in the same lesion group, respectively. Two-way ANOVA, Holm-Sidak test, $p < 0.05$. Scale bar: 100 μm in ***E*** for ***A-E***.

Figure 9. Changes in neurotrophin expression in response to partial deafferentation. ***A-O,*** BDNF, NT-3 and NGF immunoreactivity in control medial rectus motoneurons (***A-C***), after short- and long-term ATD transection (***D-F*** and ***G-I***, respectively), and after short- and long-term MLF lesion (***J-L*** and ***M-O***, respectively). Note the stronger staining in short-term images for the three neurotrophins. Motoneurons were identified by retrograde rhodamine labeling (in red, insets). ***P-R,*** Comparisons of the optical density in the cell bodies of medial rectus motoneurons between the five different groups for BDNF (***P***), NT-3 (***Q***) or NGF (***R***) staining. Control, black bar; short-term ATD, light green; long-term ATD, dark green; short-term MLF, light blue; and long-term MLF, dark blue. For ***P-R***, * indicates differences with control; # indicates differences between lesions at the same time point; ● indicates differences between time

JNeurosci Accepted Manuscript

points in the same lesion group. Two-way ANOVA, Holm-Sidak test, $p < 0.05$. For BDNF (***P***), $22 \leq n \leq 161$ cells; for NT-3 (***Q***) $24 \leq n \leq 138$ cells; and for NGF (***R***) $17 \leq n \leq 169$ cells. Scale bar: 25 μm in ***O*** for ***A***-***O***; 30 μm for the insets.

Figure 10. Schematic representation of medial rectus motoneurons innervated by MLF and ATD inputs in the control situation (***A***). Note that MLF terminals are preferentially located in dendrites, whereas ATD axons end mostly at the soma. Proper innervation leads to normal eye-related firing pattern in medial rectus motoneurons (EP, eye position; FR, firing rate). Three days after ATD transection (***B,*** 3 days postlesion ATD***,*** 3d pl ATD), ATD distal axons are suffering Wallerian degeneration. The lack of this afferent input leads to reduced firing pattern modulation related to eye displacements. The reduction in afferent synaptic information might increase neurotrophin (NT) expression in medial rectus motoneurons. This trophic signal could induce GAP-43 expression in abducens internuclear neurons, what might produce, in turn, axonal sprouting in this pathway and reinnervation of the partially deafferented motoneurons (***C***, 60 days postlesion ATD, 60 d pl ATD), and thus the recovery of the normal firing pattern.

JNeurosci Accepted Manuscript

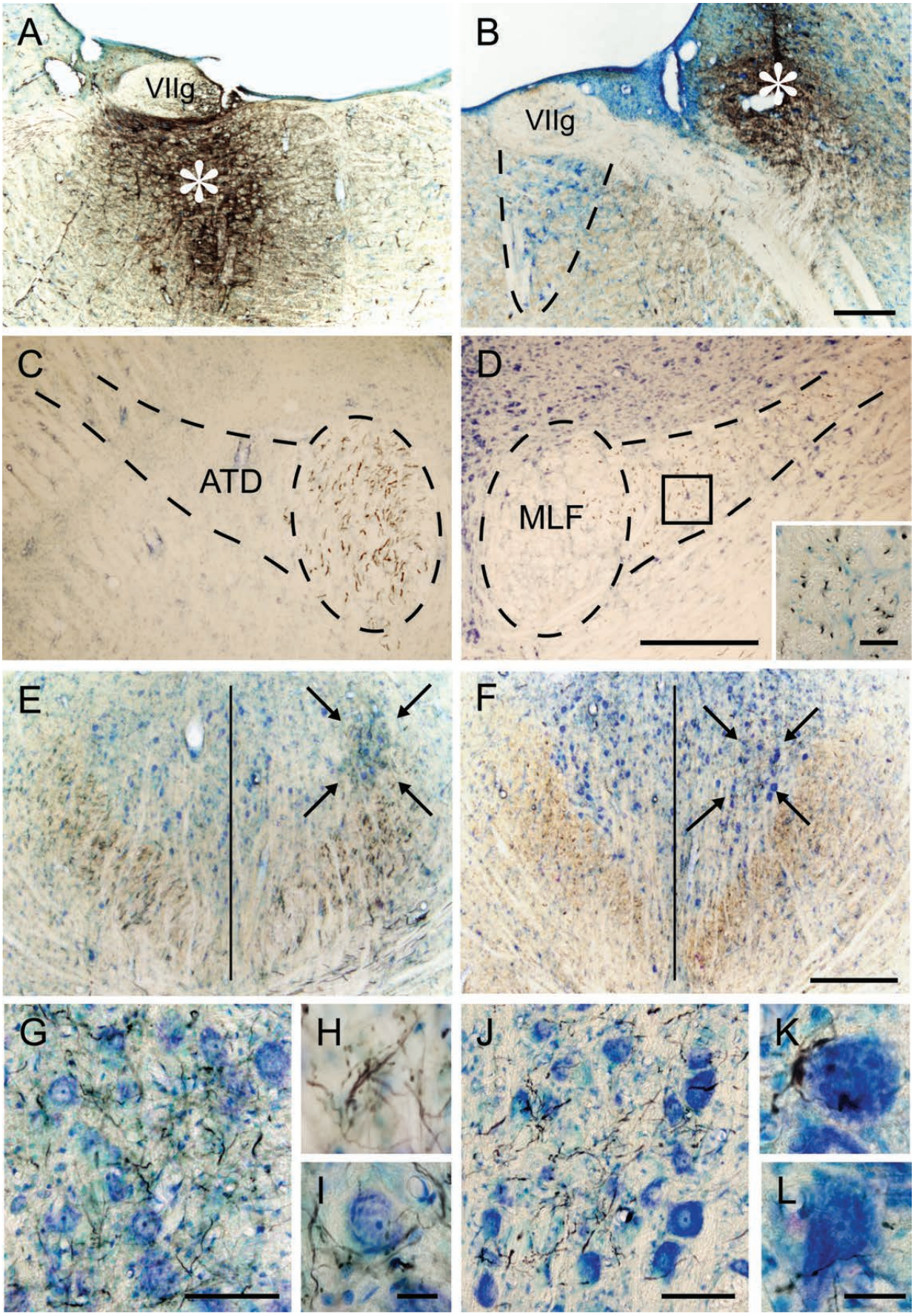

JNeurosci Accepted Manuscript

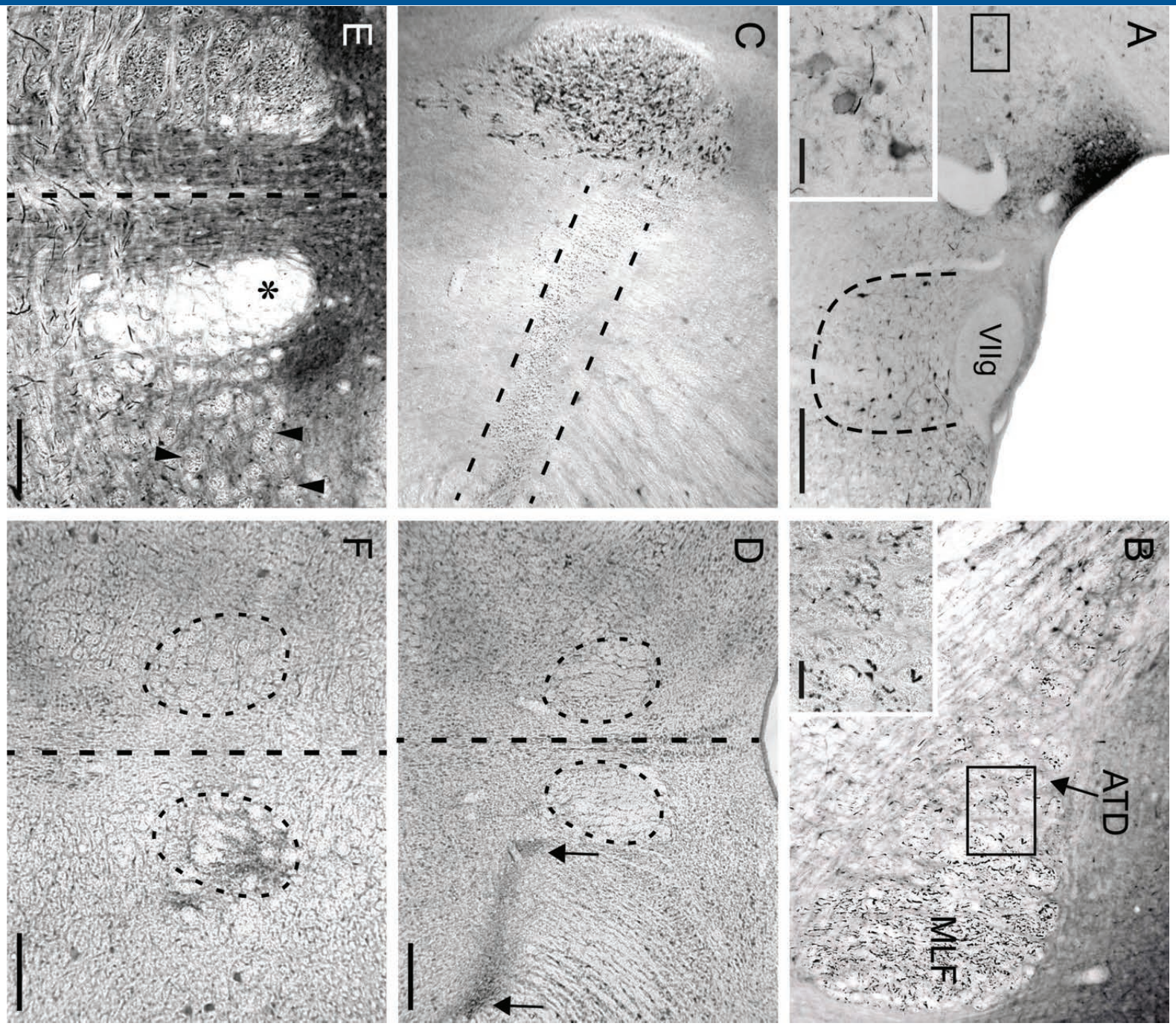

JNeurosci Accepted Manuscript

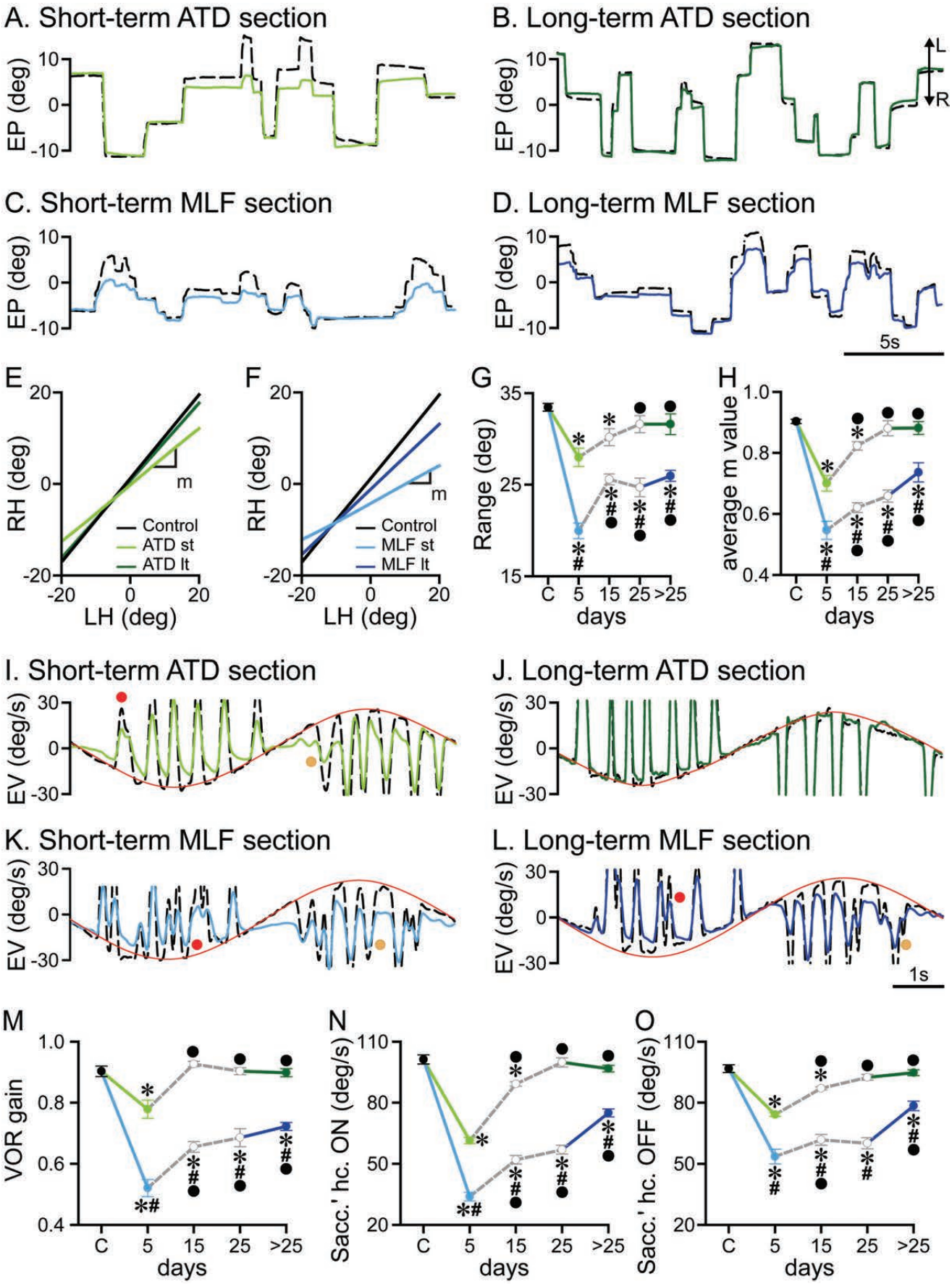

JNeurosci Accepted Manuscript

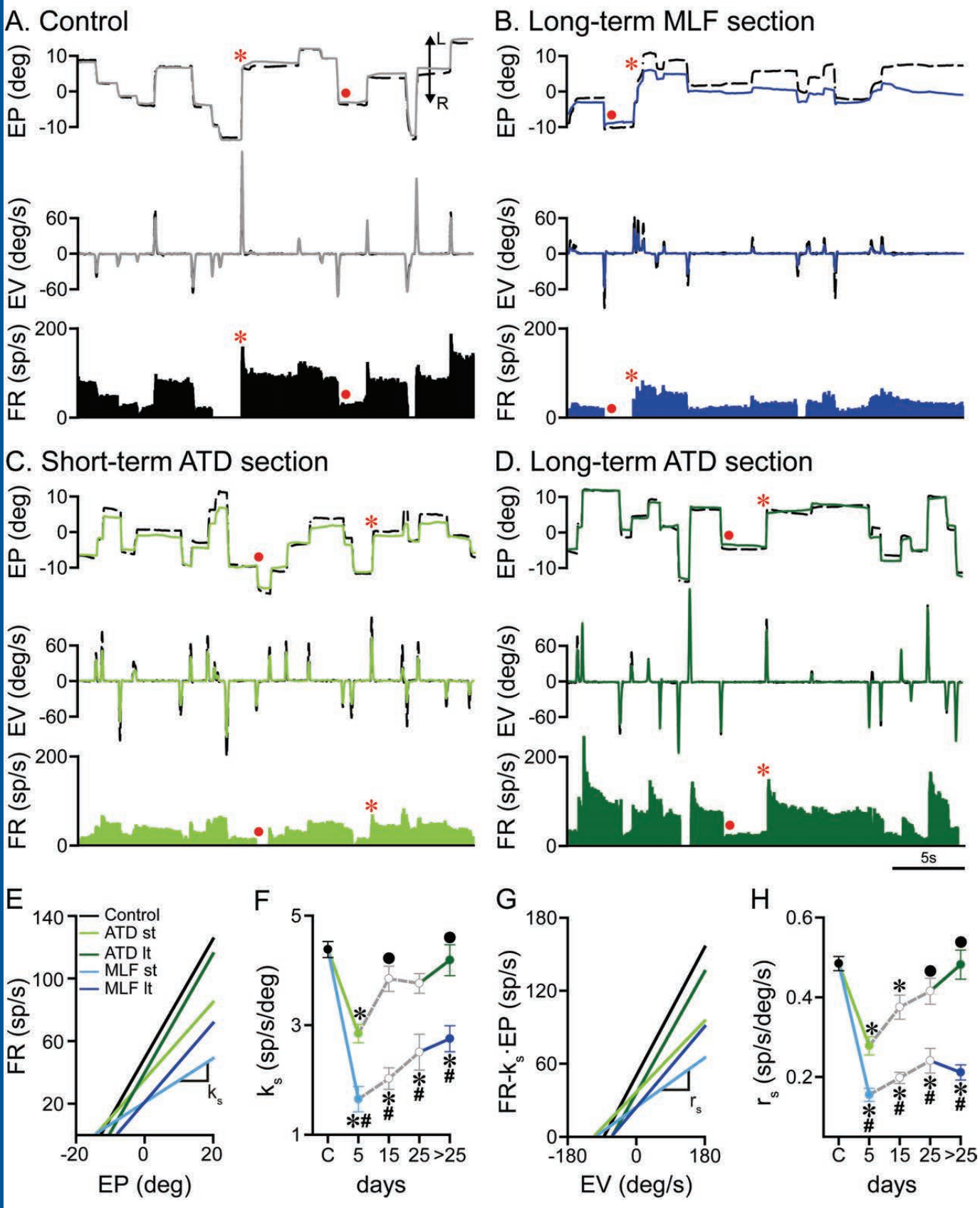

JNeurosci Accepted Manuscript

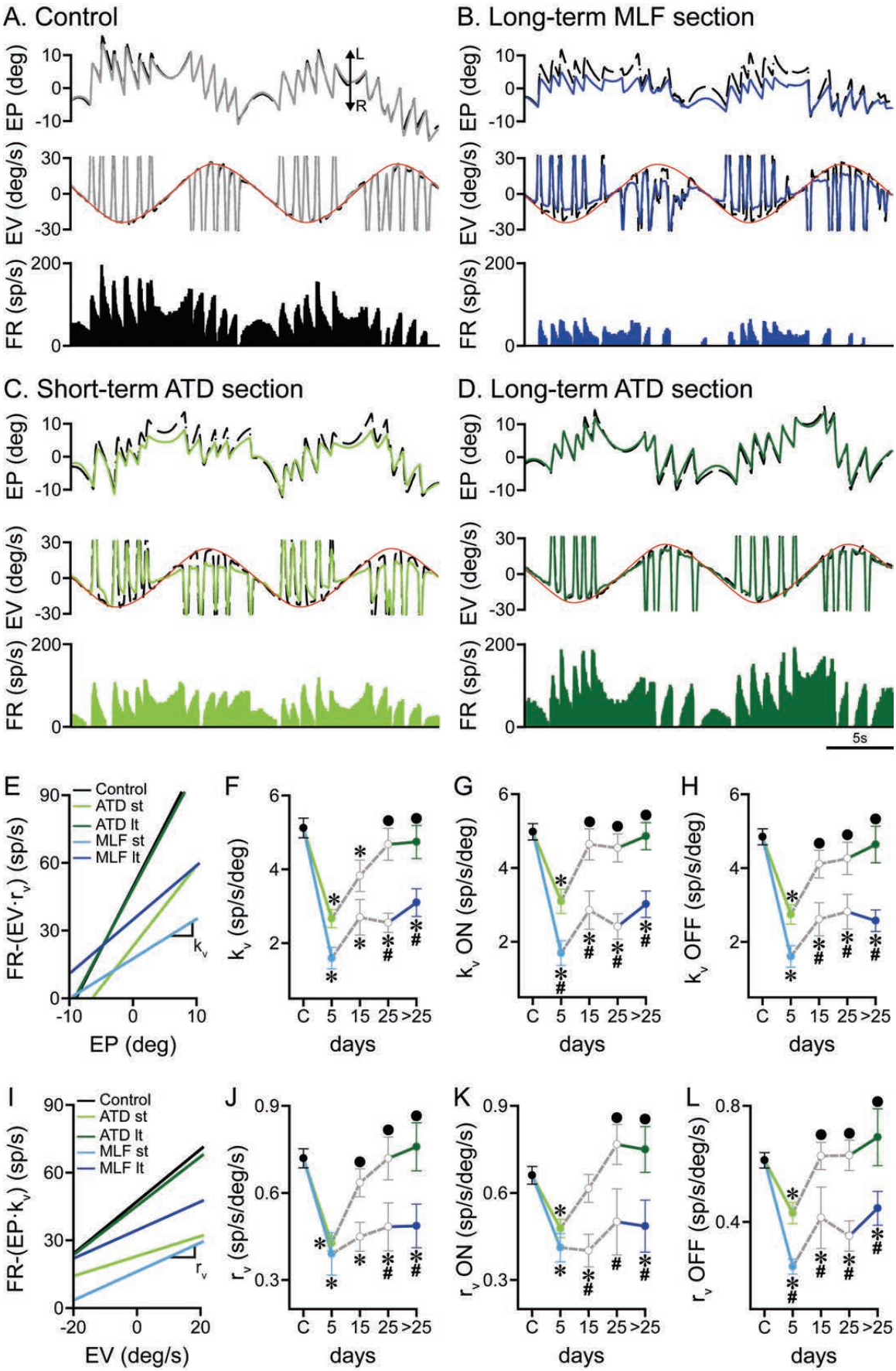

JNeurosci Accepted Manuscript

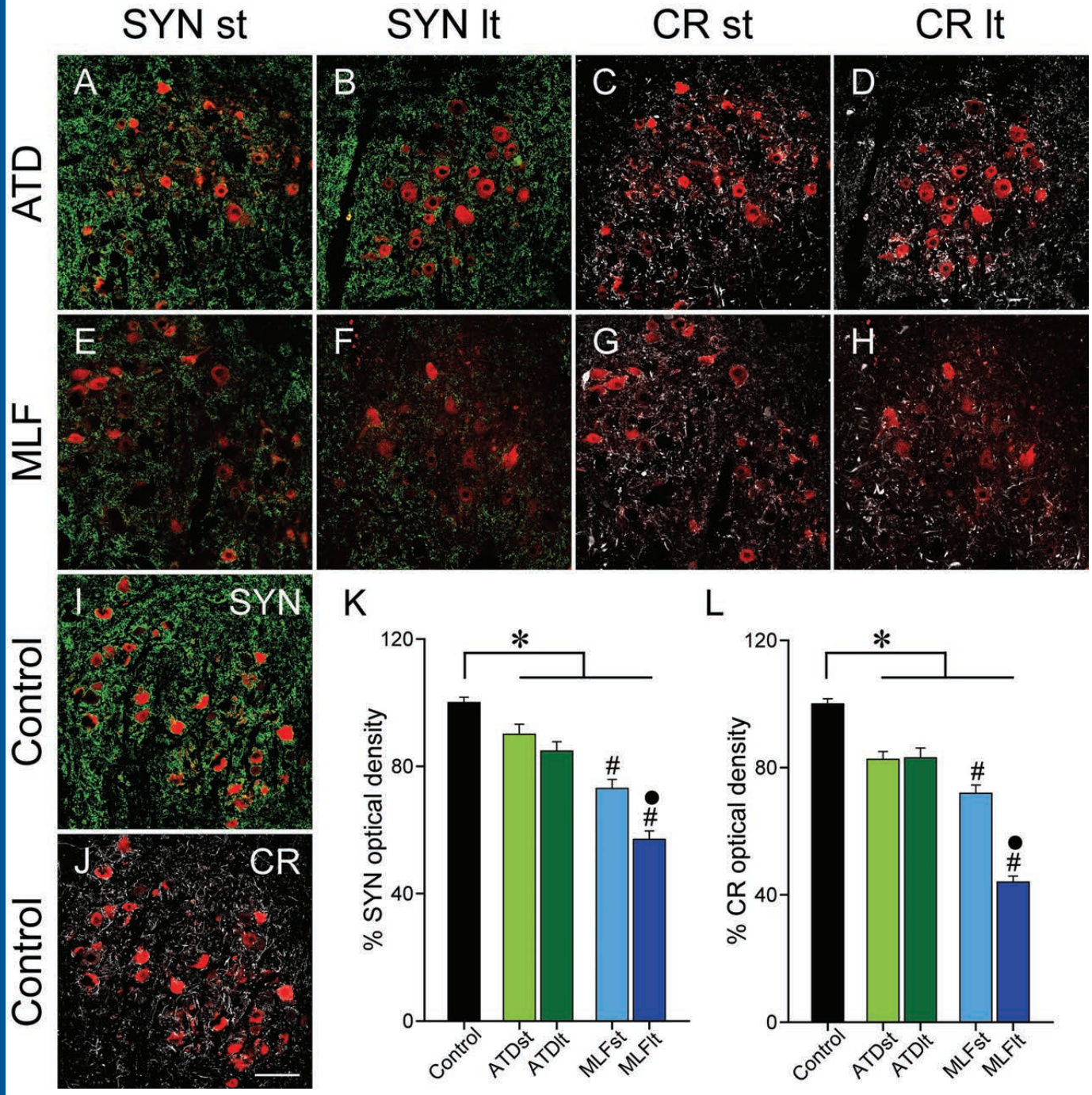

JNeurosci Accepted Manuscript

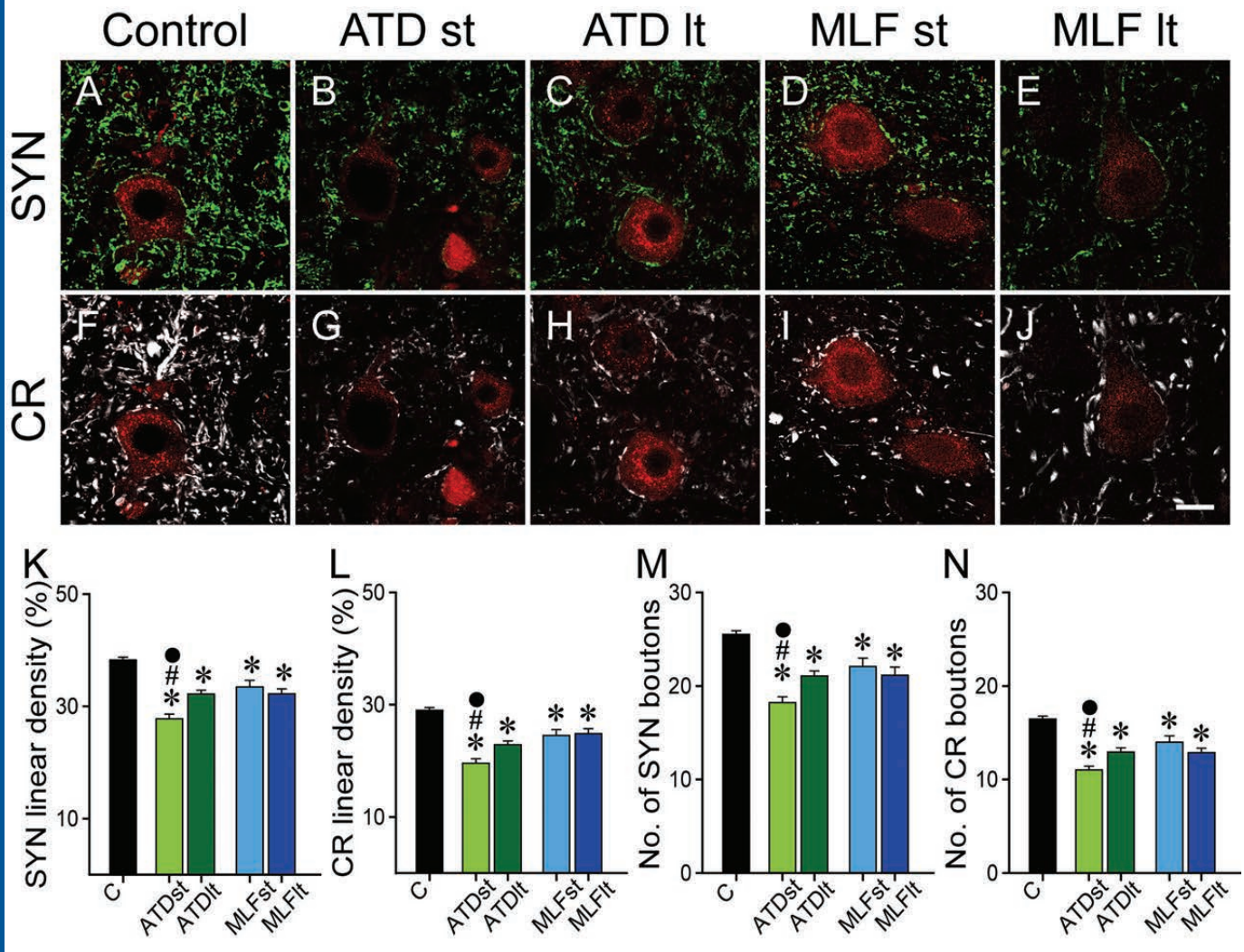

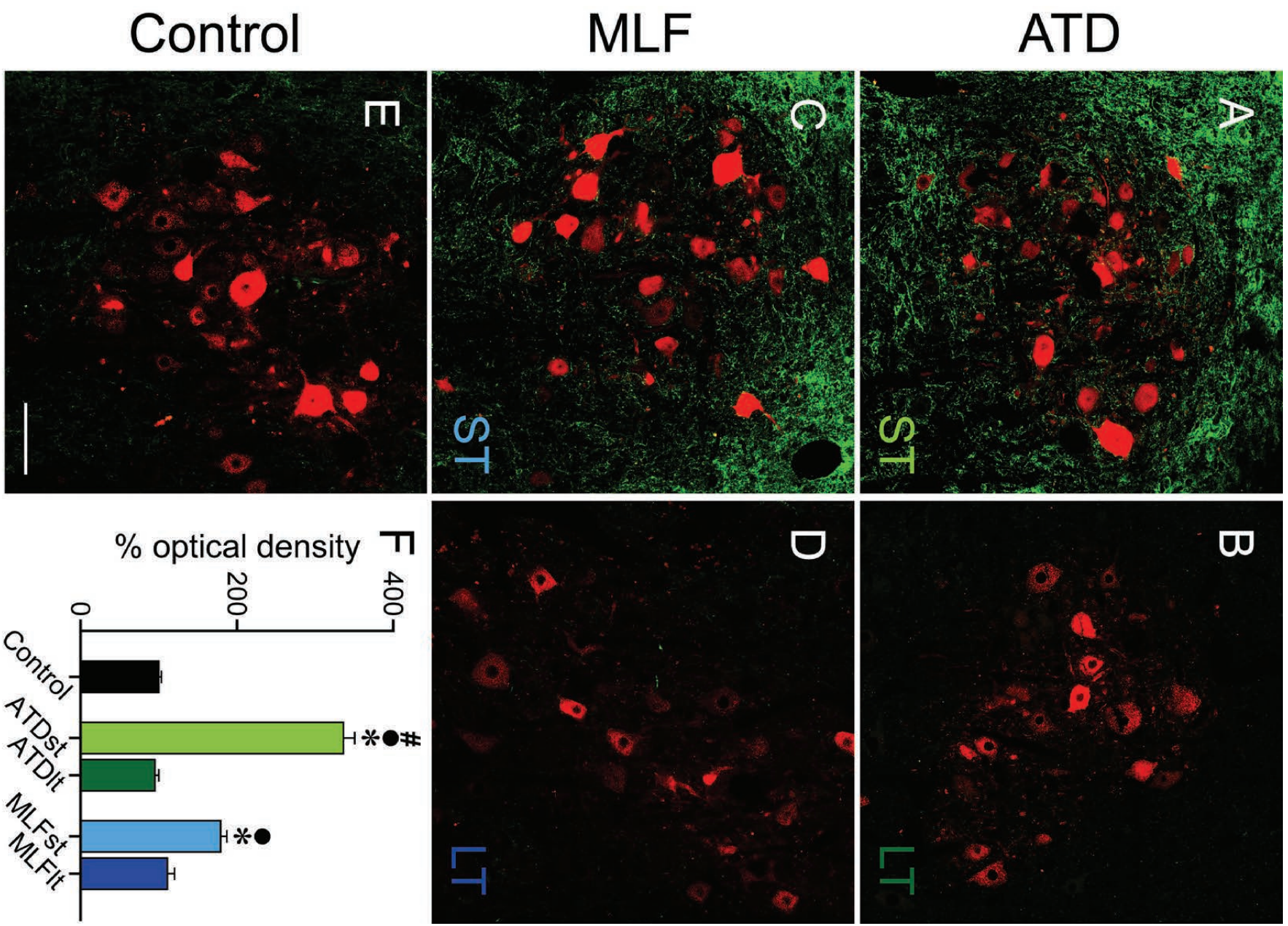
Control
MLF
ATD
E
C
A
ST
ST
D
B
LT
LT
F
% optical density
0
200
400
Control
ATDst
ATDit
MLFst
MLFit
*●#
*●

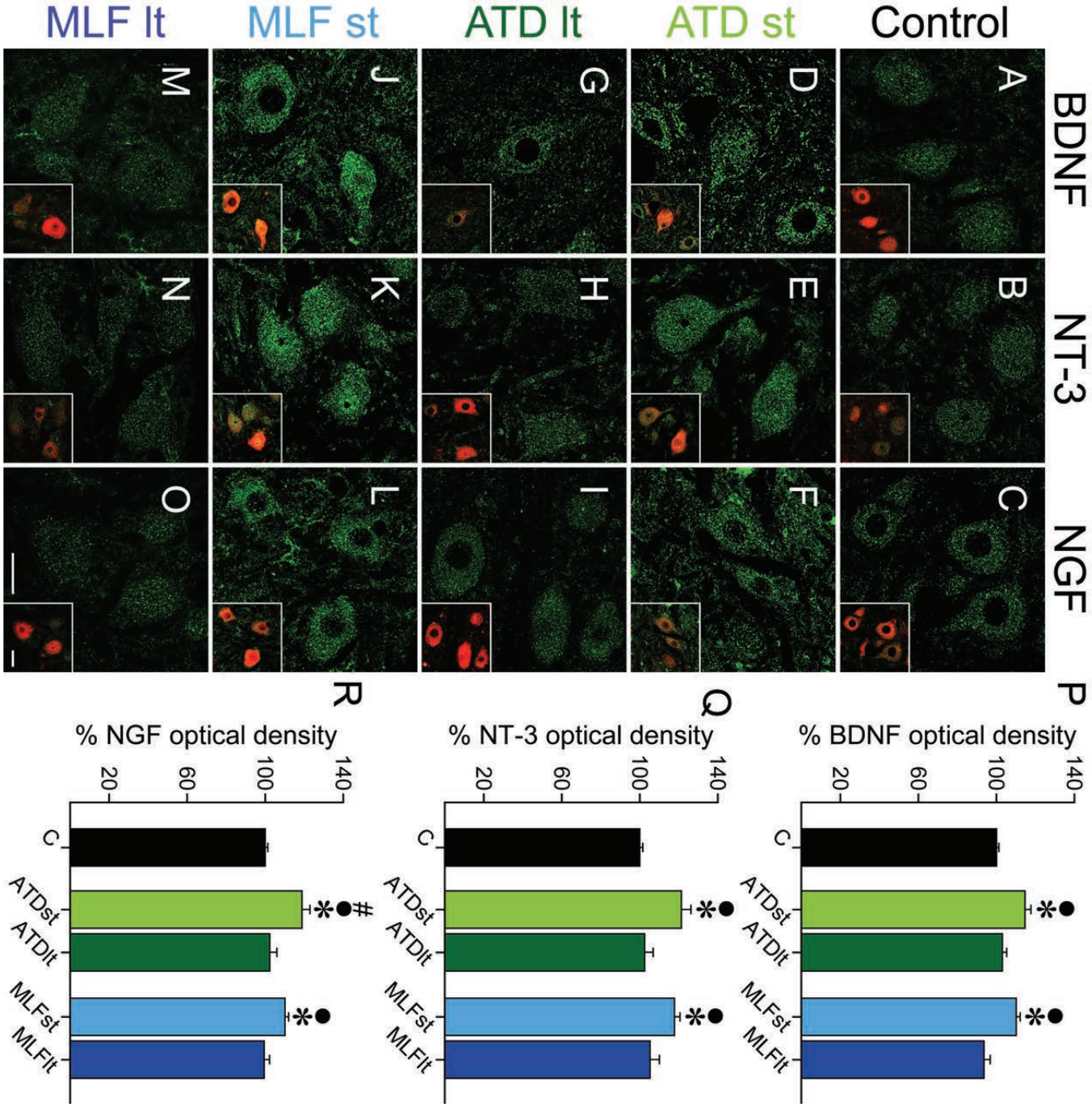
MLF lt
MLF st
ATD lt
ATD st
Control
BDNF
NT-3
NGF
A
B
C
D
E
F
G
H
I
J
K
L
M
N
O
P
% BDNF optical density
Q
% NT-3 optical density
R
% NGF optical density
20
60
100
140
C
ATDst
ATDit
MLFst
MLFit

JNeurosci Accepted Manuscript